

## Robust receding horizon parameterized control for multi-class freeway networks: A tractable scenario-based approach

Shuai Liu<sup>1,\*</sup>, Anna Sadowska<sup>1</sup>, José Ramón D. Frejo<sup>2</sup>, Alfredo Núñez<sup>3</sup>,  
Eduardo F. Camacho<sup>4</sup>, Hans Hellendoorn<sup>1</sup> and Bart De Schutter<sup>1</sup>

<sup>1</sup>*Delft Center for Systems and Control, Delft University of Technology, The Netherlands*

<sup>2</sup>*Dept. de Matemáticas e Ingeniería, Loyola University Andalusia, Spain*

<sup>3</sup>*Section of Railway Engineering, Delft University of Technology, The Netherlands*

<sup>4</sup>*Dept. de Ingeniería de Sistemas y Automática, Escuela Superior de Ingenieros, University of Seville, Spain*

### SUMMARY

In this paper, we propose a tractable scenario-based receding horizon parameterized control (RHPC) approach for freeway networks. In this approach, a scenario-based min–max scheme is used to handle uncertainties. This scheme optimizes the worst case among a limited number of scenarios that are considered. The use of parameterized control laws allows us to reduce the computational burden of the robust control problem based on the multi-class METANET model w.r.t. conventional model predictive control. To assess the performance of the proposed approach, a simulation experiment is implemented, in which scenario-based RHPC is compared with nominal RHPC, standard control ignoring uncertainties, and standard control including uncertainties. Here, the standard control approaches refer to state feedback controllers (such as PI-ALINEA for ramp metering). A queue override scheme is included for extra comparison. The results show that nominal RHPC approaches and standard control ignoring uncertainties may lead to high queue length constraint violations, and including a queue override scheme in standard control may not reduce queue length constraint violations to a low level. Including uncertainties in standard control approaches can obviously reduce queue length constraint violations, but the performance improvements are minor. For the given case study, scenario-based RHPC performs best as it is capable of improving control performance without high queue length constraint violations. Copyright © 2016 John Wiley & Sons, Ltd.

Received 5 December 2014; Revised 7 September 2015; Accepted 16 November 2015

KEY WORDS: scenario-based control; receding horizon parameterized control; min-max scheme; uncertainties; multi-class traffic

### 1. INTRODUCTION

According to different points of focus, there are various approaches for realizing traffic management. On-line model-based control approaches are receiving more and more attention in literature recently, because of their potential for improving control performance [1–4]. In on-line model-based control approaches, traffic models are critical, because they are used for determining control decisions. Macroscopic models, which are less accurate than microscopic models in general, are often used for on-line model-based traffic control in order to reduce the computational complexity with respect to microscopic models.

According to the level of aggregation, macroscopic traffic models can be divided into homogeneous models and heterogeneous models. In homogeneous models, all the vehicles are assumed to have the same characteristics, and the differences among different types of vehicles are neglected.

\*Correspondence to: Shuai Liu, Delft Center for Systems and Control, Delft University of Technology, Mekelweg 2, 2628 CD Delft, The Netherlands.

†E-mail: s.liu-1@tudelft.nl; shuailiu.tud@gmail.com

In contrast, in heterogeneous multi-class models, these differences are considered, and vehicles are divided into different classes, such as cars, trucks, vans, and so on. The density of vehicles can be maintained around a critical value corresponding to maximum flow with a single-class fundamental diagram for mixed traffic. However, for model predictive control (MPC), in which the objective function depends on the dynamics of the controlled system, a more accurate model implies better prediction of future characteristics of the controlled system; thus, the controller has better information for determining control inputs. In general, the heterogeneous multi-class models are more accurate than homogeneous single-class models, without increasing the computing complexity significantly. Some researchers have investigated the advantages of multi-class models. Wong and Wong [5] extended the Lighthill-Whitham-Richards (LWR) model to a multi-class version and found that the multi-class LWR model can reproduce some traffic phenomena (e.g., two-capacity phenomenon, hysteresis phenomenon of phase transition and platoon dispersion) that the single-class case cannot reproduce. Schreiter *et al.* [6] developed a multi-class controller that rerouted the traffic class specifically and showed that a multi-class controller outperformed a single-class controller. Liu *et al.* [7] extended METANET to a multi-class version, in which each vehicle class is assumed to be limited within its assigned space of the road, subjecting to its own fundamental diagram. Note, however, that there are interactions among different classes of vehicles, that is, the space fractions of different classes of vehicles vary with the densities of all classes of vehicles. Numerical experiments show that the multi-class METANET can improve performance more than single-class METANET. In addition, the calibration and analysis for this multi-class METANET has been done in [8], where it was fitted with data generated by a microscopic simulator VISSIM (traffic flow simulation software, PTV Planung Transport Verkehr AG, Karlsruhe, Germany) with real demands.

Various uncertainties exist in the on-line model-based control procedure for traffic networks. In particular, demand uncertainties, model uncertainties, missing samples, sensor errors, and delays are all significant factors in on-line model-based traffic control. In multi-class traffic models, the fractions of different vehicle classes in the demands at the origins of the network are needed. Thus, the uncertainties in the estimation of these fractions will affect the control performance. Considering these uncertainties in the on-line model-based control design is important for improving the control performance and for ensuring the satisfaction of constraints. In face of uncertainties in the control procedure, robust control aims to maintain the control performance within a specified range and to ensure the satisfaction of constraints. There are two strategies to realize robust control for nonlinear systems. One method is to keep the cost function to be a strictly decreasing Lyapunov function when the uncertainties are also included [9, 10]. The other method is to consider the uncertainties in the control design, where both the optimality of performance and the constraint satisfaction are considered for all possible uncertainties. The robust control problem is computationally very complex, and many approaches have been developed to deal with it. The min-max approach [11, 12], which considers the worst case among all possible uncertainties, is one of the most popular approaches. However, the min-max approach is conservative because the worst-case scenario does not always occur.

Some robust control approaches have been developed for traffic networks. Ukkusuri *et al.* [13] proposed a robust optimal traffic signal control approach for urban networks with the future demand assumed to be uncertain, and they developed a robust system-optimal control approach with an embedded cell transmission model. Similarly considering the uncertainties in the origin-destination demands, Jones *et al.* [14] proposed the near-Bayes near-Minimax method for robust traffic signal control for an urban network and obtained a good compromise solution between the Bayes case and the Minimax case. Tettamanti *et al.* [15] developed a min-max MPC approach for urban networks to minimize the objective function in the worst-case scenario. Zhong *et al.* [16] dealt with the robust control problem by using a min-max scheme and solved the optimal control for freeway networks using a set of recursive coupled Riccati difference equations. Liu *et al.* [17] developed the scenario-based RHPC approach for single-class METANET and found that the nominal RHPC approach can lead to high queue length constraint violations and the scenario-based RHPC approach can effectively reduce queue length constraint violations.

The contributions of the current paper are as follows. We propose a tractable scenario-based RHPC approach for freeway networks based on a multi-class traffic model. RHPC [18] is a variation of standard MPC, which is based on dynamic model prediction and a receding horizon approach. In MPC, the control inputs are directly optimized for the whole control horizon, and the number of variables in the optimization problem is determined by the length of the control horizon. In contrast, in RHPC, the control inputs are parameterized, and only the parameters of the control laws are optimized instead of all control inputs. These parameters can be time-varying or constant, and therefore, the number of variables in the optimization problem can be decreased with respect to the MPC case. Several parameterized laws for freeway networks are given in this paper. Moreover, we use a scenario-based scheme to deal with the robust control problem, considering a limited set of scenarios for the uncertainties to obtain the worst-case scenario, which is actually optimized in the min-max scheme. The scenario-based scheme has been discussed and analyzed in [19, 20]. The motivation for adopting this scheme is to reduce the computational complexity in comparison with other applications of robust control for traffic networks in which the worst case among all possible scenarios for the uncertainties is optimized. Intuitively, considering a limited number of scenarios for the uncertainties makes the control design method tractable relative to considering all the possible scenarios. Queue length constraints are often considered in freeway networks, and here we include a soft penalty to limit the queue lengths. The reason for not using hard constraint is to avoid infeasible optimization problems. In addition, we implement a case study and compare the scenario-based RHPC with nominal RHPC for multiple scenarios, to illustrate the effectiveness of this new approach.

This paper is organized as follows. Section 2 is about the preliminaries of this paper; this section introduces the multi-class METANET model that is used for control design in this paper, and also it gives the basic concepts of robust MPC. In Section 3, we propose the tractable scenario-based RHPC approach for freeway networks, including analysis of uncertainties, the definition of the performance index, the new RHPC laws based on the multi-class METANET model, and the development of the scenario-based RHPC approach for freeway networks. In Section 4, we implement a case study to assess the novel approach. Finally, conclusions and several future research topics are given in Section 5.

## 2. PRELIMINARIES

### 2.1. Traffic flow model: multi-class METANET

Inspired by the approach in [21] for extending the LWR model [22, 23] into a multi-class version, Liu *et al.* [8] developed a multi-class METANET model based on the single-class METANET model [24]. This multi-class METANET model is chosen as the prediction model for traffic flows in this paper. Freeway stretches are represented by links (indexed by  $m$ ), and the links are divided into several homogeneous segments (indexed by  $i$ ). The segments are described by traffic flow variables of each class (indexed by  $c$ ) of vehicles: traffic outflow of vehicles  $q_{m,i,c}(k)$  (veh/h), segmental density of vehicles  $\rho_{m,i,c}(k)$  (veh/km/h), and space-mean speed of vehicles  $v_{m,i,c}(k)$  (km/h). In addition, nodes are used for describing changes in the geometry of the roads. In our multi-class METANET model, each vehicle class is assumed to be limited within its assigned space of the road, subjecting to its own fundamental diagram. This assigned space is described by the space fraction  $\alpha_{m,i,c}$  of vehicles of class  $c$ . Note, however, that in our multi-class METANET model there are interactions among different classes of vehicles, that is, the space fractions of different classes of vehicles vary with the densities of all classes of vehicles.

The flow, density, and speed equations for vehicles of class  $c$  are as follows:

$$q_{m,i,c}(k) = \rho_{m,i,c}(k)v_{m,i,c}(k)\lambda_m \quad (1)$$

$$\rho_{m,i,c}(k+1) = \rho_{m,i,c}(k) + \frac{T}{L_m\lambda_m}(q_{m,i-1,c}(k) - q_{m,i,c}(k)) \quad (2)$$

$$\begin{aligned}
 v_{m,i,c}(k+1) = & v_{m,i,c}(k) + \frac{T}{\tau_{m,c}} \left( V_{m,c} \left( \frac{\rho_{m,i,c}(k)}{\alpha_{m,i,c}(k)} \right) - v_{m,i,c}(k) \right) \\
 & + \frac{T}{L_m} v_{m,i,c}(k) (v_{m,i-1,c}(k) - v_{m,i,c}(k)) \\
 & - \frac{T \eta_{m,c}}{L_m \tau_{m,c}} \frac{\rho_{m,i+1,c}(k) - \rho_{m,i,c}(k)}{\rho_{m,i,c}(k) + \kappa_{m,c}}
 \end{aligned} \tag{3}$$

$$V_{m,c}(\rho_{m,i,c}(k)) = v_{\text{free},m,c} \exp \left( \frac{-1}{a_{m,c}} \left( \frac{\rho_{m,i,c}(k)}{\alpha_{m,i,c}(k) \rho_{\text{crit},m,c}} \right)^{a_{m,c}} \right) \tag{4}$$

in which  $T$  is the simulation time step length,  $k$  is the simulation time step counter corresponding to the time instant  $t = kT$ ,  $\lambda_m$  is the number of lanes in link  $m$ ,  $L_m$  is the length of link  $m$ ,  $\tau_{m,c}$ ,  $\eta_{m,c}$ ,  $\kappa_{m,c}$ , and  $a_{m,c}$  are class-dependent model parameters,  $V_{m,c}(\rho_{m,i,c}(k))$  is the desired speed at density  $\rho_{m,i,c}(k)$ ,  $v_{\text{free},m,c}$  is the free-flow speed of vehicles of class  $c$  in link  $m$ , and  $\rho_{\text{crit},m,c}$  is the critical density of vehicles of class  $c$  in link  $m$ .

Moreover, dynamic speed limits can be included through the desired speed equation as follows [1]:

$$V_{m,c}(\rho_{m,i,c}(k)) = \min \left( v_{\text{free},m,c} \exp \left( \frac{-1}{a_{m,c}} \left( \frac{\rho_{m,i,c}(k)}{\alpha_{m,i,c}(k) \rho_{\text{crit},m,c}} \right)^{a_{m,c}} \right), (1 + \chi_{m,c}) v_{\text{control},m,i}(k) \right) \tag{5}$$

with  $v_{\text{control},m,i}$  the dynamic speed limit in segment  $i$  of link  $m$  and  $1 + \chi_{m,c}$  the non-compliance factor, which is used for describing the phenomenon that some drivers may violate the dynamic speed limits.

The queue length at origin  $o$  (mainstream origin or on-ramp) is described as

$$w_{o,c}(k+1) = w_{o,c}(k) + T(d_{o,c}(k) - q_{o,c}(k)) \tag{6}$$

where  $w_{o,c}$  is the queue length of vehicles of class  $c$  at the origin  $o$ ,  $d_{o,c}$  is the origin demand of vehicles of class  $c$ , and  $q_{o,c}$  is the origin outflow of vehicles of class  $c$ .

The outflow of origin  $o$  is modeled as

$$\begin{aligned}
 q_{o,c}(k) = \min \left[ & d_{o,c}(k) + \frac{w_{o,c}(k)}{T}, \alpha_{m,1,c}(k) C_{o,c} r_o(k), \right. \\
 & \left. \alpha_{m,1,c}(k) C_{o,c} \left( \frac{\rho_{\text{max},m,c} - \rho_{m,1,c}(k) / \alpha_{m,1,c}(k)}{\rho_{\text{max},m,c} - \rho_{\text{crit},m,c}} \right) \right]
 \end{aligned} \tag{7}$$

where  $\alpha_{m,1,c}$  is the space fraction of vehicles of class  $c$  in the segment that the origin  $o$  is connected to,  $\rho_{m,1,c}$  is the density of vehicles of class  $c$  in that segment,  $\rho_{\text{max},m,c}$  is the maximum density of vehicles of class  $c$  in the link  $m$  that the origin is connected to,  $C_{o,c}$  is the theoretical maximum capacity of origin  $o$  if there would be only vehicles of class  $c$ , and  $r_o$  is the ramp metering rate for on-ramp  $o$ .

In order to determine the space fractions of vehicles of class  $c$ , three traffic regimes are distinguished [8]: free flow, semi-congestion, and congestion.

*2.1.1. Free flow.* In this case, all classes of vehicles are in the free-flow regime, which means that the equivalent density of each vehicle class in its assigned space is no more than its critical density. The space fraction of vehicle class  $c$  is then taken as

$$\alpha_{m,i,c}(k) = \frac{\rho_{m,i,c}(k)}{\rho_{\text{crit},m,c}} \tag{8}$$

where  $n_c$  is the number of vehicle classes.

2.1.2. *Semi-congestion.* Here, some classes of vehicles are in the free-flow regime, while other classes of vehicles are in the congested regime. The space fractions of the vehicle classes in free flow are

$$\alpha_{m,i,c} = \frac{\rho_{m,i,c}(k)}{\rho_{\text{crit},m,c}} \quad \text{for } c \in S_{m,i,\text{free}}(k) \quad (9)$$

where  $S_{m,i,\text{free}}(k)$  is the set of all vehicle classes that are in free flow in segment  $i$  of link  $m$  at time step  $k$ . The space fractions of the congested vehicle classes are computed through the following system of equations:

$$\begin{cases} V_{m,c} \left( \frac{\rho_{m,i,c}(k)}{\alpha_{m,i,c}(k)} \right) = V_{m,l_{m,i}} \left( \frac{\rho_{m,i,l_{m,i}}(k)}{\alpha_{m,i,l_{m,i}}(k)} \right) & \text{for } c \in S_{m,i,\text{cong}}(k) / \{l_{m,i}\} \\ \sum_{c \in S_{m,i,\text{cong}}(k)} \alpha_{m,i,c}(k) = 1 - \sum_{j \in S_{m,i,\text{free}}(k)} \alpha_{m,i,j}(k) \end{cases} \quad (10)$$

where  $S_{m,i,\text{cong}}(k)$  is the set of all vehicle classes that are in congested mode in segment  $i$  of link  $m$  at time step  $k$ , and  $l_{m,i}$  is arbitrary element in  $S_{m,i,\text{cong}}(k)$ .

2.1.3. *Congestion.* All classes of vehicles are in the congested mode, and the desired speeds of all classes of vehicles are equal. The space fractions can be obtained by solving the following system of equations:

$$\begin{cases} V_{m,1} \left( \frac{\rho_{m,i,1}(k)}{\alpha_{m,i,1}(k)} \right) = V_{m,2} \left( \frac{\rho_{m,i,2}(k)}{\alpha_{m,i,2}(k)} \right) \\ \vdots \\ V_{m,n_c-1} \left( \frac{\rho_{m,i,n_c-1}(k)}{\alpha_{m,i,n_c-1}(k)} \right) = V_{m,n_c} \left( \frac{\rho_{m,i,n_c}(k)}{\alpha_{m,i,n_c}(k)} \right) \\ \sum_{c=1}^{n_c} \alpha_{m,i,c}(k) = 1 \end{cases} \quad (11)$$

For more details about the multi-class METANET model, we refer the interested reader to [8].

## 2.2. Robust control

We first give some background on robust MPC, which is the basis of deriving the scenario-based RHPC approach. Robust MPC takes uncertainties into account for determining control inputs. This is different from nominal MPC, in which the non-controllable inputs are assumed to be known, and uncertainties are neglected in the control design step.

Assume that the traffic network is described as a discrete-time nonlinear system of the following form:

$$x(k+1) = f(x(k), u(k), D(k), \omega(k)) \quad (12)$$

where  $x$  represents the system variables (e.g., density and speed),  $u$  represents the control input (e.g., ramp metering rates and dynamic speed limits),  $D$  represents the non-controllable input (e.g., demands), and  $\omega$  represents the uncertainties.

The objective function of the MPC problem is based on the prediction  $\tilde{x}(k)$  of the states over the prediction period (with length  $N_p$ ), on the control inputs  $\tilde{u}(k)$  over the control period (with length  $N_c \leq N_p$ ), and on the non-controllable input  $\tilde{D}(k)$ , which is assumed to be known or estimated via an adequate prediction model. They are defined as follows:

$$\tilde{x}(k) = [x^T(k+1), \dots, x^T(k+N_p)]^T \quad (13)$$

$$\tilde{u}(k) = [u^T(k), \dots, u^T(k+N_c-1)]^T \quad (14)$$

$$\tilde{D}(k) = [D^T(k), \dots, D^T(k + N_p - 1)]^T \quad (15)$$

where control input  $u(k + l)$  equals  $u(k + N_c - 1)$  for  $l = N_c, \dots, N_p - 1$ .

For predicting the future system states, the non-controllable inputs are usually assumed to be known nominal values in nominal MPC. Thus, the prediction states yielded by the nonlinear model are influenced by the realization  $\tilde{\omega}(k)$  of the uncertainties over the prediction period:

$$\tilde{\omega}(k) = [\omega^T(k), \dots, \omega^T(k + N_p - 1)]^T \quad (16)$$

In case the real values of the non-controllable inputs and the nominal values are significantly different, the control decisions given by nominal MPC may not satisfy the control requirements. However, the realizations of the uncertainties  $\tilde{\omega}(k)$  are not known *a priori*, and the robust MPC problem is complex if all possible scenarios of uncertainties are considered. The robust MPC problem based on the min-max scheme is formulated as follows [11]:

$$\min_{\tilde{u}(k), \tilde{x}(k)} \max_{\tilde{\omega}(k) \in \mathbb{W}} J(\tilde{x}(k), \tilde{u}(k), \tilde{D}(k), \tilde{\omega}(k)) \quad (17)$$

subject to

$$x(k + l + 1) = f(x(k + l), u(k + l), D(k + l), \omega(k + l)), \quad (18)$$

$$l = 0, 1, \dots, N_p - 1,$$

$$x(k) = x_k, \quad (19)$$

$$u(k + l) = u(k + N_c - 1), \quad l = N_c, \dots, N_p - 1, \quad (20)$$

$$x(k + l) \in \mathbb{X}, \quad l = 1, 2, \dots, N_p, \quad (21)$$

$$u(k + l) \in \mathbb{U}, \quad l = 0, 1, \dots, N_c - 1 \quad (22)$$

$$\text{for all } \tilde{\omega}(k) \in \mathbb{W}$$

where  $x_k$  represents the state at time step  $k$ ,  $\mathbb{W}$  represents the set of all the possible realizations of uncertainties over the prediction horizon,  $\mathbb{X}$  is the set containing all the feasible states, and  $\mathbb{U}$  is the set containing all the feasible control inputs.

According to the receding horizon scheme, only the first element  $u(k)$  of optimal input sequence  $\tilde{u}(k)$  is applied to the traffic network. After that, the prediction horizon shifts to the next control step, and the control inputs are optimized again. For the robust problem consisting of (17)–(22), computational complexity increases rapidly as the size of traffic network grows, making the problem intractable in practice. As a solution, we propose a novel tractable scenario-based RHPC approach for freeway networks.

### 3. TRACTABLE SCENARIO-BASED RHPC FOR FREEWAY NETWORKS

#### 3.1. Uncertainties in freeway networks

The non-controllable inputs ( $\tilde{D}$ ) in on-line model-based control for freeway networks include the mainstream demands, on-ramp demands, boundary conditions, etc. As an example, let us here consider the uncertainties in the traffic demand, including the uncertainties in the total value of demand and the fractions of different classes of vehicles in the demand. Note, however, that other types of uncertainties can also be dealt with the scenario-based RHPC approach.

The nominal demand can be estimated in various ways, based on the historical data and on-line measurement data. An intuitive way is that the nominal demand is estimated as the average of historical data. Considering the difference among different weekdays and weekends; the nominal demand

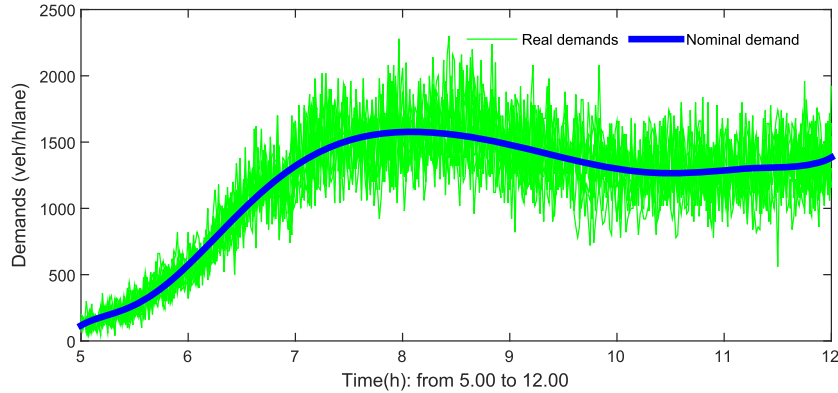


Figure 1. An example of real demands and nominal demand.

can be estimated separately from Monday to Sunday. Thus, the characteristics of different weekdays and weekends can be described more accurately. Moreover, if on-line measurements are available, shifting and scaling the nominal demand according to these measurements can also improve the estimation. In addition, another way is to build a library of possible uncertainties and their possibilities of appearance.

The measured total mainstream demands of the Dutch A13 freeway near Rijswijk on several Fridays in 2013 and 2014 are shown in Figure 1. The real demands are plotted with the same linetype and these real demand profiles overlap with each other. Based on these demands, a nominal demand is estimated as the average of these historical real demands and shown in Figure 1 with a different linetype. This figure shows that real demands fall within a confidence band around the nominal demand. Thus, it makes sense to model the uncertainties in the total demand as noise limited by a certain lower bound and upper bound.

The estimations of the fractions of different classes of vehicles can be obtained in a similar way as the estimation of the total demand profile. However, the estimations of these fractions ask for separate measurements for different vehicle classes, which requires cameras to be installed along freeway stretches. Because of economic reasons and practicability, installing cameras in high density in a freeway network is not that common yet. Therefore, the uncertainties in the estimation of the fractions of different classes of vehicles are nonnegligible in robust control for freeway networks based on multi-class traffic models.

### 3.2. Performance index for freeway networks

The Total Time Spent (TTS) represents the total time that all vehicles spend in the traffic network. In on-line model-based control for freeway networks, the TTS is often used as performance index. Here, we also use it as the performance index, but it is important to note that other performance indices such as total emissions can also be included according to the aim of the traffic control. Ramp Metering (RM) and Variable Speed Limits (VSL) are chosen as control measures, because they are efficient in decreasing TTS and easy to realize [25, 26].

In this paper, as an example, the multi-class METANET model is used as the prediction model, and  $TTS^{\ddagger}$  can be defined as follows:

$$TTS(k_c) = T \sum_{j=k_c M}^{(k_c + N_p)M-1} \sum_{c=1}^{n_c} p_c \left( \sum_{(m,i) \in I_{\text{all}}} \rho_{m,i,c}(j) L_m \lambda_m + \sum_{o \in O_{\text{all}}} w_{o,c}(j) \right) \quad (23)$$

<sup>‡</sup>Note that the TTS index here includes the TTS for all segments, the TTS for all origins, and the TTS for all on-ramps, and they are treated equally, that is, their weights are equal to 1.

in which  $k_c$  is the control time step counter corresponding to the time instant  $t = k_c T_c$ ,  $T_c$  is the control time step length,<sup>§</sup>  $n_c$  is the number of vehicle classes,  $I_{\text{all}}$  is the set of the indices of all pairs of segments and links,  $O_{\text{all}}$  is the set including the indices of all origins, and  $p_c$  represents the passenger car equivalents (pce) for vehicle class  $c$ :

$$p_c = \frac{L_c}{L_{\text{car}}} \tag{24}$$

where  $L_c$  is the length of vehicles of class  $c$ , and  $L_{\text{car}}$  is the length of the reference class car.

Without including uncertainties, the objective function can be defined as

$$J(k_c) = \xi_{\text{TTS}} \frac{\text{TTS}(k_c)}{\text{TTS}_{\text{nom}}} + \frac{\xi_{\text{ramp}}}{N_c N_{\text{ramp}}} \sum_{j=k_c}^{k_c+N_c-1} \sum_{o \in O_{\text{ramp}}} \|r_o^{\text{ctrl}}(j) - r_o^{\text{ctrl}}(j-1)\| + \frac{\xi_{\text{speed}}}{N_c N_{\text{VSL}}} \sum_{j=k_c}^{k_c+N_c-1} \sum_{(m,i) \in I_{\text{speed}}} \left\| \frac{v_{m,i}^{\text{ctrl}}(j) - v_{m,i}^{\text{ctrl}}(j-1)}{v_{\text{free},m,\text{max}}} \right\| \tag{25}$$

in which  $\text{TTS}_{\text{nom}}$  is the TTS value for some nominal control profile,  $r_o^{\text{ctrl}}(k_c)$  is the ramp metering rate at origin  $o$  at control step  $k_c$ ,  $r_o(k) = r_o^{\text{ctrl}}(k_c)$  for  $k = Mk_c + 1, \dots, (M+1)k_c$ ,  $v_{m,i}^{\text{ctrl}}(k_c)$  is the variable speed limit in segment  $i$  of link  $m$  at control step  $k_c$ ,  $v_{\text{control},m,i}(k) = v_{m,i}^{\text{ctrl}}(k_c)$  for  $k = Mk_c + 1, \dots, M(k_c + 1)$  with  $M = T_c/T$  assumed to be an integer,  $v_{\text{free},m,\text{max}}$  is the maximum free-flow speed among all classes of vehicles in link  $m$ ,  $O_{\text{ramp}}$  includes all metered origins,  $I_{\text{speed}}$  includes all the segments with speed limits,  $\xi_{\text{TTS}}$ ,  $\xi_{\text{ramp}}$  and  $\xi_{\text{speed}}$  are positive weights,  $N_{\text{ramp}}$  is the number of metered on-ramps, and  $N_{\text{VSL}}$  is the number of variable speed limits. In the objective function (25), the second term and the third term are used for penalizing the variations of the control inputs. The second and third terms would limit the freedom for fully optimizing the first term. However, in general, the extent to which this occurs is case-dependent and cannot be determined a priori.

Note that the three terms in (25) are all normalized, so that they have the same magnitude if their weights are all the same ( $\xi_{\text{TTS}} = \xi_{\text{ramp}} = \xi_{\text{speed}}$ ). The first term is normalized with nominal TTS, which is taken as the TTS for the case without control and uncertainties here. The second term includes  $N_c$  control time steps and  $N_{\text{ramp}}$  metered on-ramps, and ramp metering rates are within  $[0, 1]$ . Thus, the second term is normalized by  $N_c N_{\text{ramp}}$ . The third term includes  $N_c$  control time steps and  $N_{\text{VSL}}$  variable speed limits, which are within  $[0, v_{\text{free},m,\text{max}}]$ . Hence, the third term is normalized by  $N_c N_{\text{VSL}} v_{\text{free},m,\text{max}}$ . In addition, setting low weights for the last two terms can make the performance index TTS dominate in the objective function.

### 3.3. Receding horizon parameterized control laws for freeway networks

The RHPC approach for traffic networks has been developed by Zegeye *et al.* [18] based on a receding horizon control scheme and parameterized control laws for single-class traffic models. 't Hart [27] also investigated some parameterized MPC laws for freeway networks based on single-class traffic model. In the RHPC approach, the control inputs are parameterized as a function of traffic states, and the parameters in these control laws are optimized instead of the full input sequence  $\tilde{u}(k_c)$ . As an extension of [18, 27], here, we present new RHPC laws for freeway networks based on multi-class models:

$$v_{m,i}^{\text{ctrl}}(k_c + 1) = \theta_{m,i,0}(k_c) v_{\text{free},m,\text{max}} + \theta_{m,i,1}(k_c) \sum_{c=1}^{n_c} \beta_{m,i,c}(k_c) \frac{v_{m,i+1,c}(k_c) - v_{m,i,c}(k_c)}{v_{m,i+1,c}(k_c) + \kappa_v} + \theta_{m,i,2}(k_c) \sum_{c=1}^{n_c} \beta_{m,i,c}(k_c) \frac{\frac{\rho_{m,i+1,c}(k_c)}{\alpha_{m,i+1,c}(k_c)} - \frac{\rho_{m,i,c}(k_c)}{\alpha_{m,i,c}(k_c)}}{\frac{\rho_{m,i+1,c}(k_c)}{\alpha_{m,i+1,c}(k_c)} + \kappa_\rho} \tag{26}$$

<sup>§</sup>Note that in Section 2, we assume  $T_c = T$ . Now, we consider the general case with  $T_c \neq T$ .

$$\begin{aligned}
 v_{m,i}^{\text{ctrl}}(k_c + 1) &= \theta_{m,i,0}(k_c)v_{\text{free},m,\text{max}} + \theta_{m,i,1}(k_c) \sum_{c=1}^{n_c} \beta_{m,i,c}(k_c) \frac{V_{m,c}(\rho_{m,i,c}(k_c)) - v_{m,i,c}(k_c)}{V_{m,c}(\rho_{m,i,c}(k_c)) + \kappa_v} \\
 &\quad + \theta_{m,i,2}(k_c) \sum_{c=1}^{n_c} \beta_{m,i,c}(k_c) \frac{\frac{\rho_{m,i+1,c}(k_c)}{\alpha_{m,i+1,c}(k_c)} - \frac{\rho_{m,i,c}(k_c)}{\alpha_{m,i,c}(k_c)}}{\frac{\rho_{m,i+1,c}(k_c)}{\alpha_{m,i+1,c}(k_c)} + \kappa_\rho} \tag{27}
 \end{aligned}$$

$$\begin{aligned}
 v_{m,i}^{\text{ctrl}}(k_c + 1) &= \theta_{m,i,0}(k_c)v_{\text{free},m,\text{max}} \\
 &\quad + \theta_{m,i,1}(k_c) \sum_{c=1}^{n_c} \beta_{m,i,c}(k_c) \frac{v_{m,i+1,c}(k_c) \frac{\rho_{m,i+1,c}(k_c)}{\alpha_{m,i+1,c}(k_c)} - v_{m,i,c}(k_c) \frac{\rho_{m,i,c}(k_c)}{\alpha_{m,i,c}(k_c)}}{v_{m,i+1,c}(k_c) \frac{\rho_{m,i+1,c}(k_c)}{\alpha_{m,i+1,c}(k_c)} + \kappa_v \kappa_\rho} \tag{28}
 \end{aligned}$$

$$\begin{aligned}
 v_{m,i}^{\text{ctrl}}(k_c + 1) &= v_{m,i}^{\text{ctrl}}(k_c) - \theta_{m,i,1}(k_c) \sum_{c=1}^{n_c} \beta_{m,i,c}(k_c)(v_{m,i,c}(k_c) - v_{m,i,c}(k_c - 1)) \\
 &\quad + \theta_{m,i,2}(k_c) \sum_{c=1}^{n_c} \beta_{m,i,c}(k_c)(V_{m,c}(\rho_{m,i,c}(k_c)) - v_{m,i,c}(k_c)) \tag{29}
 \end{aligned}$$

$$r_o^{\text{ctrl}}(k_c + 1) = r_o^{\text{ctrl}}(k_c) + \theta_{o,1}(k_c) \sum_{c=1}^{n_c} \beta_{m,1,c}(k_c) \frac{\rho_{\text{crit},m,c} - \frac{\rho_{m,1,c}(k_c)}{\alpha_{m,1,c}(k_c)}}{\rho_{\text{crit},m,c}} \tag{30}$$

$$\begin{aligned}
 r_o^{\text{ctrl}}(k_c + 1) &= r_o^{\text{ctrl}}(k_c) - \theta_{o,1}(k_c) \sum_{c=1}^{n_c} \beta_{m,1,c}(k_c)(\rho_{m,1,c}(k_c) - \rho_{m,1,c}(k_c - 1)) \\
 &\quad + \theta_{o,2}(k_c) \sum_{c=1}^{n_c} \beta_{m,1,c}(k_c)(\rho_{\text{crit},m,c} - \rho_{m,1,c}(k_c)) \tag{31}
 \end{aligned}$$

where  $\beta_{m,i,c}(k_c) = \frac{\rho_{m,i,c}(k_c)}{\sum_{j=1}^{n_c} \rho_{m,i,j}(k_c)}$  is the density fraction of vehicles of class  $c$  in segment  $i$  of link  $m$ , the index  $m$  in (30) and (31) represents the link that is connected to the on-ramp  $o$ , the index 1 represents the first segment of that link,  $\kappa_v$  and  $\kappa_\rho$  are small positive values to prevent the divisors to be 0, and  $\theta_{m,i,0}$ ,  $\theta_{m,i,1}$ ,  $\theta_{m,i,2}$ ,  $\theta_{o,1}$  and  $\theta_{o,2}$  are the control parameters that are optimized in the control process.

*Remark 1*

In (26)–(31), these control parameters are varying over the control horizon. Thus, the control inputs (variable speed limits and ramp metering rates) vary with both the control parameters and the traffic states. The following considerations about these control parameters can be made:

- The control parameters in the RHPC laws are not necessarily optimized at every control time step (i.e., every  $T_c$ ). This will introduce a new control time step (different from  $T_c$ ) for updating the control parameters for RHPC. However, for simplifying the exposition, we just assume that these control parameters in the RHPC laws are optimized at every control time step (i.e., every  $T_c$ ) in this paper.
- These control parameters can be assumed to be constant during the prediction horizon ( $[k_c T_c, (k_c + N_p) T_c]$ ), which covers the control horizon ( $[k_c T_c, (k_c + N_c) T_c]$ ). Thus, the control inputs (variable speed limits and ramp metering rates) vary only with the traffic states. In this case, the number of variables in the optimization problem to be solved is reduced with respect to the case with varying control parameters.
- For a traffic network, the control parameters for different segments and on-ramps can be grouped, for example, the parameters for the segments of the same link can be assumed to be equal. Then the number of variables in the optimization problem to be solved is reduced with respect to the case that the control parameters are not grouped.

The RHPC laws (26)–(31) are constructed based on the traffic states of the current segment and the next segment, which reflect future traffic situation for vehicles in the current segment. Inspired by the speed equation of METANET, Law (26) consists of the free-flow speed, the relative variation in the speed from the current segment to the next segment, and the relative variation in the equivalent density from the current segment to the next segment at the current control step. Compared with Law (26), the second term of Law (27) is the relative difference between the *desired* speed and the actual speed in the current segment at the current control step. Law (28) includes the free-flow speed and the relative variation in the flow from the current segment to the next segment at the current control step. With the *desired* speed and actual speeds as inputs, Law (29) is inspired by the PI-ALINEA law for ramp metering [28]. Law (30) is a generalization of the ALINEA law [29], and Law (31) is a generalization of the PI-ALINEA law [28].

For all the RHPC laws here, the integration of different classes of vehicles is based on a convex combination with density fractions of different vehicle classes as weights. Directly using independent parameters for different vehicle classes could be a generalization of the way of including the traffic states of all classes of vehicles in (26)–(31).

Note that there may be some instability in the speed equation of METANET. In MPC for nonlinear systems according to literature [30–32], the instability in the controlled system can be addressed through making the prediction horizon large enough or by including an end-point constraint. In our work, we make the prediction horizon large enough. In addition, the Courant-Friedrichs-Lewy [33] condition is often considered as the condition for the stability of traffic flow models (e.g., METANET). More specifically, no vehicle can cross a segment in one simulation time step [34], that is, the simulation time step is chosen based on the principle

$$T < \min_{m \in I_{\text{link}}} \frac{L_m}{\max_{c=1, \dots, n_c} v_{\text{free}, m, c}} \quad (32)$$

where  $I_{\text{link}}$  represents the set including all links, and  $\max_{c=1, \dots, n_c} v_{\text{free}, m, c}$  is the free-flow speed of the fastest class of vehicles for the link  $m$ .

#### Remark 2

The RHPC laws (26)–(31) are independent from the traffic flow model that is used in this paper. Even if the multi-class METANET model is replaced by some other traffic flow model, these laws can still be adopted.

The following constraint conditions<sup>¶</sup> are used for ensuring the control inputs stay within their upper bounds and lower bounds:

$$v_{m,i}^{\text{ctrl}}(k_c + 1) = \max(\min(v_{m,i}^{\text{ctrl}}(k_c + 1), v_{\max, m}), v_{\min, m}) \quad (33)$$

$$r_o^{\text{ctrl}}(k_c + 1) = \max(\min(r_o^{\text{ctrl}}(k_c + 1), r_{\max, o}), r_{\min, o}) \quad (34)$$

in which  $v_{\max, m}$  and  $v_{\min, m}$  are respectively the upper bound and lower bound of the variable speed limits in link  $m$ , and  $r_{\max, o}$  and  $r_{\min, o}$  are respectively the upper bound and lower bound of the ramp metering rate at origin  $o$ .

#### 3.4. Scenario-based receding horizon parameterized control

In order to obtain optimal control inputs in RHPC for freeway networks, traffic state variables need to be predicted with future demands as exogenous inputs. Nominal RHPC for freeway networks adapts nominal demands, which may be very different from the real demands. This difference may affect the control performance and the constraint satisfaction. Here, we propose a tractable scenario-based RHPC approach, aiming to improve the behavior of the controlled system by

<sup>¶</sup>Note that these constraints are hard constraints for control inputs, and they are directly included in the control procedure.

taking the uncertainties into account. The worst-case scenario among a limited number of scenarios is optimized to realize the control objective. This scenario-based scheme is used for reducing the computational burden. Moreover, in order to aim at the satisfaction of the queue length constraints, we include a queue length penalty, which is a soft constraint as in [35]. The objective function of the tractable scenario-based RHPC approach is as follows:

$$\begin{aligned}
 J_{\min\text{-max}}(\tilde{x}(k_c), \tilde{u}(k_c), \tilde{D}(k_c)) = \max_{\tilde{\omega}(k_c) \in \tilde{\Omega}(k_c)} & \left\{ J(\tilde{x}(k_c), \tilde{u}(k_c), \tilde{D}(k_c), \tilde{\omega}(k_c)) \right. \\
 & \left. + \gamma \sum_{o \in O_{\text{ramp}}} \max \left( \frac{\max_{j=k_c M, \dots, (k_c + N_p) M - 1} \sum_{c=1}^{n_c} p_c w_{o,c}(j)}{w_{\max,o}} - 1, 0 \right) \right\} \quad (35)
 \end{aligned}$$

where  $\tilde{\Omega}(k_c) = \{\tilde{\omega}_1(k_c), \dots, \tilde{\omega}_H(k_c)\} \subset \mathbb{W}$  represents the set of  $H$  possible scenarios that will be considered for the scenario-based RHPC approach for control time step  $k_c$ ,  $w_{\max,o}$  is the maximum queue length (in pce) allowed at on-ramp  $o$ , and  $\gamma$  is a positive weight to penalize queue length constraint violation under uncertainties  $\tilde{\omega}(k_c) \in \tilde{\Omega}(k_c)$ .

The scenario-based RHPC problem for freeway networks is defined as follows:

$$\begin{aligned}
 \min_{\tilde{u}(k_c), \tilde{x}(k_c)} & J_{\min\text{-max}}(\tilde{x}(k_c), \tilde{u}(k_c), \tilde{D}(k_c)) \quad (36) \\
 \text{subject to} & (18)\text{--}(22) \text{ for all } \tilde{\omega}(k_c) \in \tilde{\Omega}(k_c)
 \end{aligned}$$

In the above scenario-based RHPC problem, when the maximum queue length is smaller than the maximum permitted value, the queue length penalty equals 0; thus, the TTS is optimized. However, if the maximum queue length is larger than the maximum permitted value, the queue length penalty will be taken into account. Because of the high weight  $\gamma$  for the queue length penalty, the queue length will be in general optimized so that the maximum queue length is smaller than the maximum permitted value. The inner max operator of the queue length penalty ensures that once the maximum queue length in the entire prediction horizon is larger than the maximum permitted value, the queue length penalty will be taken into account.

#### 4. CASE STUDY

##### 4.1. Benchmark network

The benchmark network shown in Figure 2, which has been simulated with other controllers in some papers [1, 36], is used for the case study. This network includes one mainstream origin, one on-ramp, one destination, and two links. Link 1 is 4 km long and divided into four segments with a length of 1 km. Link 2 is 2 km long and divided into two segments with a length of 1 km. Thus, the length of the segments for both links is  $L_m = 1$  km for  $m = 1, 2$ . The on-ramp connects to the first segment of link 2. There are two lanes in the main road, and one lane in the on-ramp road. It is assumed that the queue length at the origin is not limited, and the outflow at the destination is unrestricted. Note that at the origin, the vehicles that cannot enter the network in one simulation step are considered to be in the origin queue, and they are taken into account together with the mainstream demand, that is, all demands are taken into account. In the third and fourth segments of link 1, variable speed limits are present, and ramp metering is used at the on-ramp.

We consider two classes of vehicles in the network: class 1 represents cars, and class 2 represents trucks. The parameters for these two classes of vehicles are as follows [1, 21, 35]:  $v_{\text{free},m,1} = 106$  km/h,  $a_{m,1} = 1.6761$ ,  $\chi_{m,1} = 0.12$ ,  $\rho_{\text{crit},m,1} = 35$  veh/km/lane,  $\rho_{\text{max},m,1} = 175$  veh/km/lane,

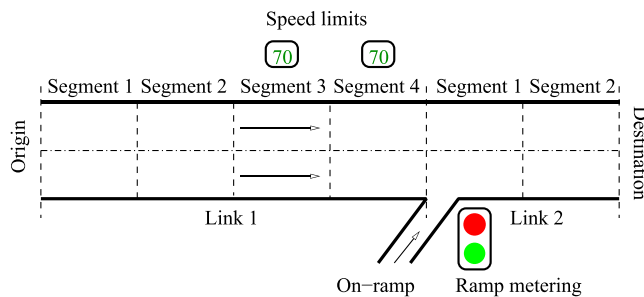


Figure 2. Benchmark network.

and  $C_{\text{mainstream},1} = 2034$  veh/h/lane for  $m = 1, 2$ ;  $v_{\text{free},m,2} = 83$  km/h,  $a_{m,2} = 2.1774$ ,  $\chi_{m,2} = 0.05$ ,  $\rho_{\text{crit},m,2} = 19$  veh/km/lane,  $\rho_{\text{max},m,2} = 75$  veh/km/lane, and  $C_{\text{mainstream},2} = 990$  veh/h/lane for  $m = 1, 2$ .

Common parameters for cars and trucks are [1, 35]:  $\tau_{m,c} = 18$  s,  $\kappa_{m,c} = 40$  veh/h/km, and  $\eta_{m,c} = 60$  km<sup>2</sup>/h for  $c = 1, 2$  and  $m = 1, 2$ . The passenger car equivalents are  $p_1 = 1$  and  $p_2 = 7/3$ . In order to avoid spillback to the upstream of the on-ramp, the total queue length (denoted by  $w_{\text{ramp}}^{\text{total}}$ ) of cars and trucks at the on-ramp is limited to 150 pce.

The simulation time step is  $T = 10$  s (according to (32),  $T < \frac{L_m}{v_{\text{free},m,1}} = 34$  s). As for other parameters, we select  $\xi_{\text{TTS}} = 1$ ,  $\xi_{\text{ramp}} = \xi_{\text{speed}} = 0.1$ ,  $T_c = 60$  s, and  $N_p = 7$ . Here, we suppose that the weights  $\xi_{\text{TTS}}$ ,  $\xi_{\text{ramp}}$ , and  $\xi_{\text{speed}}$  are defined by policymakers. The performance index TTS dominates in the objective function, and the penalties to avoid abrupt variations in control inputs are minor in comparison with TTS. The weight  $\gamma$  is tested for different values: 0.01, 0.1, 1, 10, 100. The control time step is six times larger than the simulation time step, because the control inputs should not be changed too frequently in practice. The control parameters for RHPC laws depend on the future predictions. Hence, the prediction horizon is not too long to avoid large prediction errors under certainties. However, the prediction horizon cannot be too short due to the requirement for crossing the traffic network within the prediction horizon. Thus, the length of the prediction horizon is chosen according to the typical travel time through the network as suggested in [1]. Note that in this case study, we assume that the parameters of the RHPC laws are constant over the entire prediction horizon, and they are different for segment 3 and segment 4 of link 1. For the parameters in the RHPC laws, the control horizon covers one control step, while for the actual control inputs, the control horizon covers seven control steps, because of the variations of the traffic states used in the RHPC laws.

#### 4.2. Control settings

The nominal demands at the mainstream origin and the on-ramp are shown in Figure 3. The nominal density fraction for trucks is  $\beta_{\text{truck}} = 0.1$ . The real demands are generated by adding random disturbances to the nominal demands. Here, we consider two cases:

- Case 1: there are only uncertainties in the total demands;
- Case 2: there are uncertainties in both the total demands and the estimations of truck fractions.

The uncertainties in the total demand values are limited within 10% with a base value of 100 veh/h. As for the truck fractions, we assume that the range is from 0 to 0.3. Both uncertainties for the total demands and for the truck fractions are uniform random noise. For each case, ten scenarios for uncertainties, corresponding to ten realizations of demands, were investigated to verify the effectiveness of the scenario-based RHPC approach.

Both the nominal RHPC and the scenario-based RHPC are implemented for comparison. In the scenario-based RHPC, ten uniform random uncertainty scenarios are used for obtaining the worst-case objective function. These ten uncertainty scenarios are different from the aforementioned ten realizations of demands. This is because of real realizations of future demands that are not known

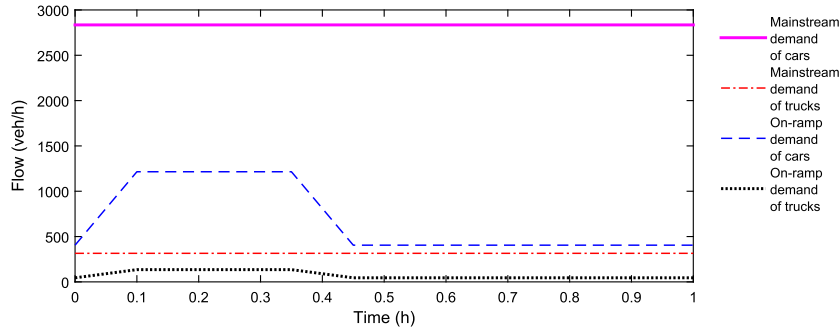


Figure 3. Nominal demands for the benchmark network.

in previous and not possible to be used in the control procedure. However, the uncertainty scenarios used in the scenario-based RHPC are generated in the same way as the aforementioned ten realizations of demands.

As examples, the RHPC laws (26) and (29) for variable speed limits and (30) and (31) for ramp metering rates are adopted in the case study. We test and compare the following approaches for the aforementioned two cases of uncertainties in the case study:

- Nominal RHPC 1 (NRHPC 1): Law (26) + Law (30);
- Scenario-based RHPC 1 (SRHPC 1): Law (26) + Law (30);
- Nominal RHPC 2 (NRHPC 2): Law (29) + Law (31);
- Scenario-based RHPC 2 (SRHPC 2): Law (29) + Law (31);

For comparison, we also implement a standard control scheme for the combination: Law (29) + Law (31), which are PI-ALINEA-like laws. In the standard control scheme, the parameters for the RHPC laws are constant for the entire simulation period, and they are determined beforehand. For the standard control scheme, we consider two cases, of which one is queue length penalty without queue override scheme<sup>||</sup> [37], and the other is queue length penalty with queue override scheme. Note that (33) and (34) are also used here. For the standard control scheme, the following approaches are tested:

- Standard control 1 (SC 1): using nominal demands with queue length penalty;
- Standard control 2 (SC 2): using ten random scenarios for uncertainties with queue length penalty;
- Standard control 3 (SC 3): based on nominal demands with queue length penalty and queue override scheme;
- Standard control 4 (SC 4): based on ten random scenarios for uncertainties with queue length penalty and queue override scheme.

#### 4.3. Results and analysis

In the remainder of this section,  $J_{\text{imp}}^{\text{TTS}}$  represents the relative improvement in TTS w.r.t. the non-control case, while  $J_{\text{pen}}$  represents the relative queue length constraint violation<sup>\*\*</sup>:

$$J_{\text{pen}} = \max \left( \frac{\max_{k=1, \dots, k_{\text{end}}} \sum_{c=1}^{n_c} [p_c w_{o,c}(k)]}{w_{\text{max},o}} - 1, 0 \right), \quad (37)$$

<sup>||</sup>In the queue override scheme, the ramp metering rate is set to be 1 if the maximum queue length exceeds the maximum permitted value.

<sup>\*\*</sup>Note that the queue length constraint violation is based on joint control through both variable speed limits and ramp metering.

Table I. Simulation results for NRHPC 1 and SRHPC 1, Case 1.

Approaches		NRHPC 1					SRHPC 1				
		$\gamma$	0.01	0.1	1	10	100	0.01	0.1	1	10
Average	$J_{imp}^{TTS}$	7.4%	6.7%	6.5%	6.4%	6.2%	6.6%	6.1%	6.0%	5.9%	5.8%
	$J_{pen}$	25.5%	9.0%	7.7%	6.6%	5.5%	13.4%	2.3%	1.9%	1.8%	1.6%
	$J_{tot}$	15.4	15.6	15.6	16.3	21.2	15.6	15.7	15.7	15.9	17.3
Standard deviation	$J_{imp}^{TTS}$	0.3%	0.4%	0.4%	0.3%	0.2%	0.5%	0.4%	0.3%	0.3%	0.3%
	$J_{pen}$	2.5%	1.2%	1.3%	2.2%	2.1%	2.1%	0.4%	0.3%	0.2%	0.3%
	$J_{tot}$	0.2	0.3	0.3	0.5	2.3	0.3	0.3	0.3	0.3	0.4

NRHPC, nominal receding horizon parameterized control; SRHPC, scenario-based receding horizon parameterized control.

Table II. Simulation results for NRHPC 1 and SRHPC 1, Case 2.

Approaches		NRHPC 1					SRHPC 1				
		$\gamma$	0.01	0.1	1	10	100	0.01	0.1	1	10
Average	$J_{imp}^{TTS}$	6.1%	4.4%	4.7%	4.6%	4.6%	4.7%	4.3%	4.3%	4.2%	4.1%
	$J_{pen}$	53.4%	21.5%	12.7%	11.2%	10.6%	18.2%	2.5%	1.6%	1.2%	1.0%
	$J_{tot}$	18.9	20.9	19.3	20.3	29.7	19.1	19.2	19.3	19.4	20.3
Standard deviation	$J_{imp}^{TTS}$	0.3%	1.2%	0.3%	0.3%	0.3%	0.2%	0.2%	0.2%	0.2%	0.3%
	$J_{pen}$	4.0%	19.5%	4.2%	2.7%	2.8%	5.3%	1.0%	0.8%	0.7%	0.6%
	$J_{tot}$	0.4	5.6	0.4	0.5	3.0	0.4	0.4	0.4	0.4	0.7

NRHPC, nominal receding horizon parameterized control; SRHPC, scenario-based receding horizon parameterized control.

Table III. Simulation results for NRHPC 2 and SRHPC 2, Case 1.

Approaches		NRHPC 2					SRHPC 2				
		$\gamma$	0.01	0.1	1	10	100	0.01	0.1	1	10
Average	$J_{imp}^{TTS}$	9.5%	5.3%	5.1%	5.1%	5.0%	9.4%	5.0%	5.0%	5.2%	5.2%
	$J_{pen}$	70.0%	4.5%	3.0%	4.0%	3.8%	66.3%	0.8%	0.8%	0.8%	0.6%
	$J_{tot}$	15.0	15.8	15.8	16.2	19.7	15.1	15.8	15.9	16.0	16.4
Standard deviation	$J_{imp}^{TTS}$	0.9%	0.2%	0.3%	0.3%	0.2%	0.7%	0.2%	0.3%	0.3%	0.3%
	$J_{pen}$	8.4%	1.2%	1.5%	2.0%	1.1%	7.1%	0.6%	0.5%	0.3%	0.4%
	$J_{tot}$	0.3	0.3	0.2	0.2	1.1	0.3	0.2	0.2	0.6	0.5

NRHPC, nominal receding horizon parameterized control; SRHPC, scenario-based receding horizon parameterized control.

Table IV. Simulation results for NRHPC 2 and SRHPC 2, Case 2.

Approaches		NRHPC 2					SRHPC 2				
		$\gamma$	0.01	0.1	1	10	100	0.01	0.1	1	10
Average	$J_{imp}^{TTS}$	7.2%	4.2%	4.0%	4.0%	4.0%	6.3%	3.9%	3.7%	3.7%	3.7%
	$J_{pen}$	125.7%	12.5%	10.1%	8.7%	9.1%	82.0%	2.7%	1.4%	1.0%	0.8%
	$J_{tot}$	18.7	19.3	19.4	20.1	28.4	18.8	19.3	19.4	19.5	20.2
Standard deviation	$J_{imp}^{TTS}$	0.5%	0.3%	0.2%	0.2%	0.2%	0.6%	0.2%	0.3	0.2%	0.2%
	$J_{pen}$	22.3%	5.4%	2.6%	2.9%	2.9%	17.5%	1.8%	0.8%	0.6%	0.3%
	$J_{tot}$	0.4	0.4	0.4	0.6	3.1	0.4	0.4	0.4	0.5	0.4

NRHPC, nominal receding horizon parameterized control; SRHPC, scenario-based receding horizon parameterized control.

where  $k_{\text{end}}$  is the last simulation time step of the entire simulation period, and the total performance  $J_{\text{tot}}$  is defined as

$$J_{\text{tot}} = \frac{\text{TTS}_{\text{tot}}}{\text{TTS}_{\text{nom}}} + \gamma J_{\text{pen}} \tag{38}$$

where  $\text{TTS}_{\text{tot}}$  is the total time spent over the entire simulation period. For each combination of the values of  $\gamma$  (five values), the realizations for uncertainties (ten scenarios), and the control approaches (eight control approaches), the simulation with control is repeated ten times with different random seeds. For each combination, the average of the results for these ten simulations is considered. The average performance improvement and the average constraint violation of those average results for ten different realizations for uncertainties are listed in Tables I–VIII. In order to show the difference for different scenarios, the standard deviations of the results for these ten different realizations are also included.

Table V. Simulation results for SC 1 and SC 2, Case 1.

Approaches		SC 1					SC 2				
		$\gamma$	0.01	0.1	1	10	100	0.01	0.1	1	10
Average	$J_{\text{imp}}^{\text{TTS}}$	6.1%	11.5%	2.2%	4.1%	6.0%	12.1%	12.1%	1.9%	1.6%	2.2%
	$J_{\text{pen}}$	114.2%	86.2%	62.6%	52.9%	70.0%	93.3%	90.0%	0%	0%	0.1%
	$J_{\text{tot}}$	29.8	14.8	16.9	21.3	85.6	14.7	14.7	16.3	16.4	16.4
Standard deviation	$J_{\text{imp}}^{\text{TTS}}$	1.6%	0.5%	2.8%	1.9%	0.3%	0.3%	0.4%	0.2%	0.2%	0.2%
	$J_{\text{pen}}$	18.9%	6.1%	45.5%	28.5%	8.9%	5.7%	5.8%	0%	0%	0.2%
	$J_{\text{tot}}$	44.8	0.2	0.5	2.6	9.1	0.2	0.3	0.2	0.2	0.4

SC, standard control.

Table VI. Simulation results for SC1 and SC2, Case 2.

Approaches		SC 1					SC 2				
		$\gamma$	0.01	0.1	1	10	100	0.01	0.1	1	10
Average	$J_{\text{imp}}^{\text{TTS}}$	6.1%	8.7%	1.9%	2.6%	6.1%	9.3%	1.0%	0.9%	1.3%	0.4%
	$J_{\text{pen}}$	241.0%	167.9%	104.5%	82.1%	151.0%	173.2%	0%	0%	1.3%	1.1%
	$J_{\text{tot}}$	18.9	18.5	20.8	27.8	169.9	18.2	19.8	19.9	20.0	21.1
Standard deviation	$J_{\text{imp}}^{\text{TTS}}$	1.2%	0.4%	2.2%	0.6%	0.4%	0.6%	0.1%	0.2%	0.3%	0.4%
	$J_{\text{pen}}$	38.4%	35.0%	65.1%	25.4%	11.8%	31.0%	0%	0%	3.0%	3.1%
	$J_{\text{tot}}$	0.5	0.4	0.5	2.7	12.0	0.4	0.4	0.5	0.6	3.2

SC, standard control.

Table VII. Simulation results for SC3 and SC4, Case 1.

Approaches		SC 3					SC 4				
		$\gamma$	0.01	0.1	1	10	100	0.01	0.1	1	10
Average	$J_{\text{imp}}^{\text{TTS}}$	2.0%	4.2%	-1.9%	1.0%	1.9%	4.6%	4.6%	2.8%	0.7%	2.3%
	$J_{\text{pen}}$	13.5%	12.2%	6.6%	6.7%	6.9%	7.9%	14.1%	0.6%	0.5%	0%
	$J_{\text{tot}}$	16.3	16.0	17.0	17.2	23.2	15.9	15.9	16.2	16.6	16.3
Standard deviation	$J_{\text{imp}}^{\text{TTS}}$	1.2%	0.2%	1.0%	0.4%	0.7%	1.0%	0.6%	0.7%	1.0%	0.2%
	$J_{\text{pen}}$	2.9%	3.8%	4.1%	3.5%	3.8%	4.0%	2.3%	1.9%	1.2%	0%
	$J_{\text{tot}}$	0.4	0.2	0.3	0.3	4.1	0.3	0.3	0.3	0.3	0.2

SC, standard control.

Table VIII. Simulation results for SC3 and SC4, Case 2.

Approaches	$\gamma$	SC 3					SC 4				
		0.01	0.1	1	10	100	0.01	0.1	1	10	100
Average	$J_{imp}^{TTS}$	1.1%	3.5%	-1.2%	0.6%	1.6%	3.8%	2.7%	1.8%	1.0%	1.5%
	$J_{pen}$	21.4%	26.2%	8.3%	10.1%	14.0%	27.7%	16.7%	0.4%	0%	0%
	$J_{tot}$	19.9	19.4	20.4	21.0	33.8	19.3	19.6	19.7	19.9	19.8
Standard deviation	$J_{imp}^{TTS}$	0.6%	0.3%	1.2%	0.3%	0.6%	0.4%	0.5%	0.3%	0.2%	0.2%
	$J_{pen}$	7.0%	7.8%	4.0%	4.9%	6.6%	4.1%	5.2%	1.3%	0%	0%
	$J_{tot}$	0.5	0.4	0.6	0.7	7.0	0.4	0.4	0.4	0.4	0.4

SC, standard control.

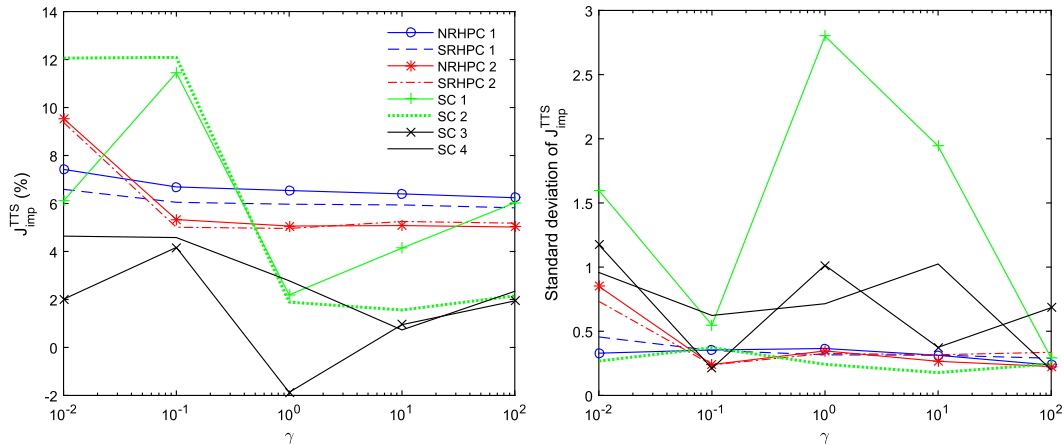


Figure 4. Performance improvements for total time spent, Case 1.

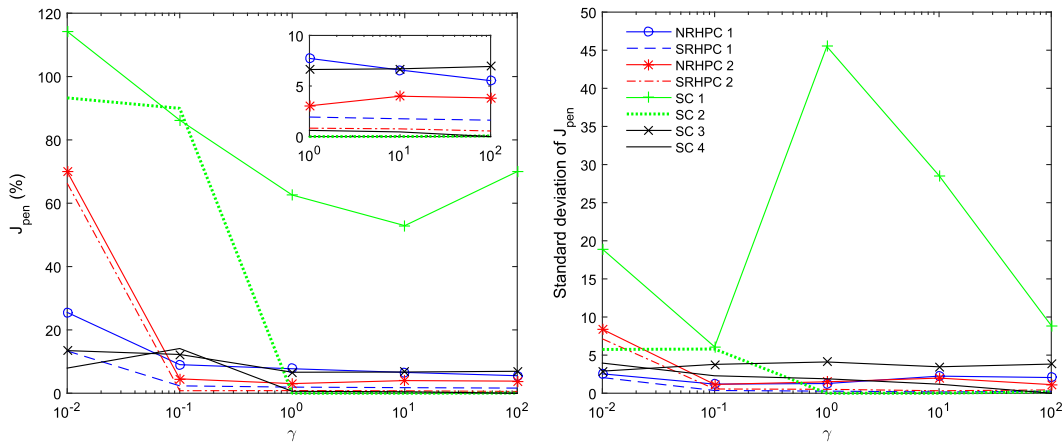


Figure 5. Constraint violations, Case 1 (with  $J_{pen}$  zoomed in for  $\gamma \in \{1, 10, 100\}$ ).

4.3.1. Comparison w.r.t. performance and constraint violations. In this section, the approaches ignoring uncertainties are first compared with the corresponding approaches including uncertainties with the same control laws, i.e., NRHPC 1 w.r.t. SRHPC 1, NRHPC 2 w.r.t. SRHPC 2, SC 1 w.r.t. SC 2, and SC 3 w.r.t. SC 4. After that, all approaches are compared together based on Figures 4–9, which display the performance improvements for TTS, constraint violations, and total performance.

(1) Results for NRHPC 1 and SRHPC 1:

According to the results for Case 1 in Table I, the performance improvements for SRHPC 1 (5.8%–6.6%) are less than the performance improvements for NRHPC 1 (6.2%–7.4%).

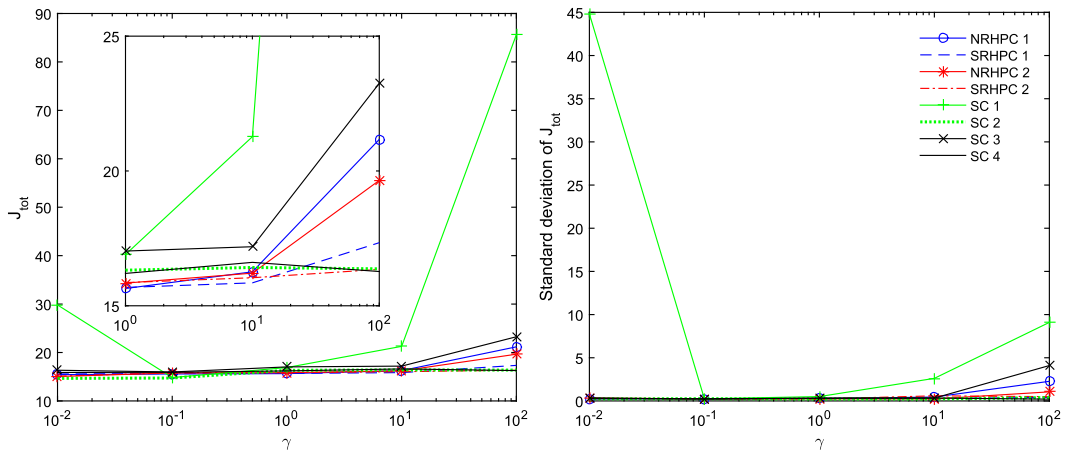


Figure 6. Total performance, Case 1 (with  $J_{tot}$  zoomed in for  $\gamma \in \{1, 10, 100\}$ ).

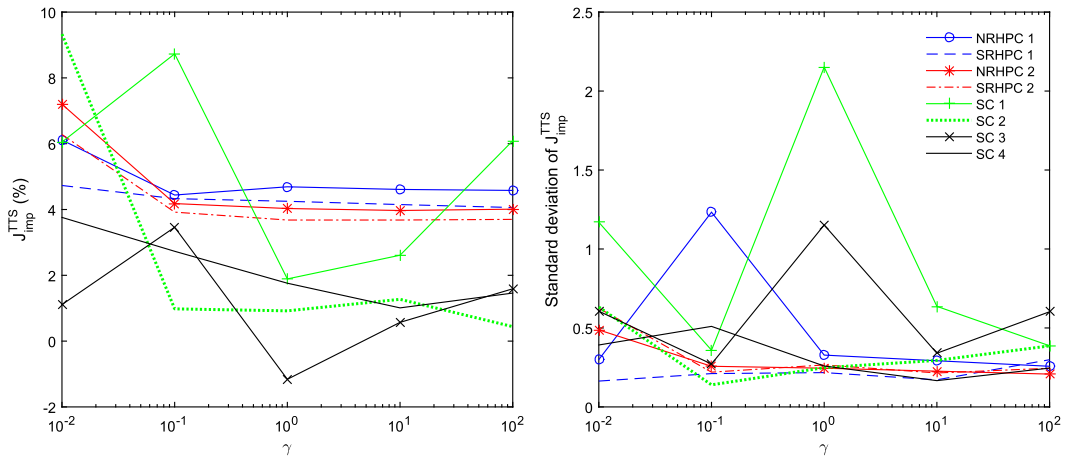


Figure 7. Performance improvements for total time spent, Case 2.

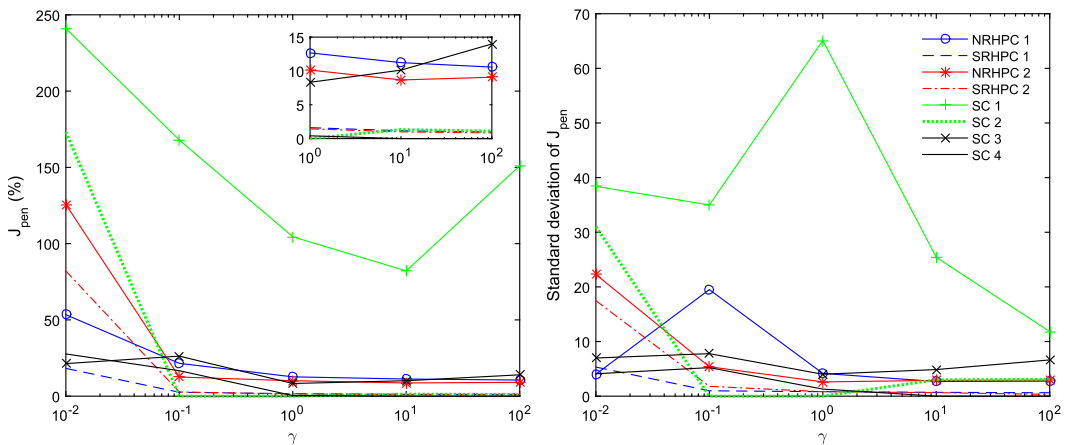


Figure 8. Constraint violations, Case 2 (with  $J_{pen}$  zoomed in for  $\gamma \in \{1, 10, 100\}$ ).

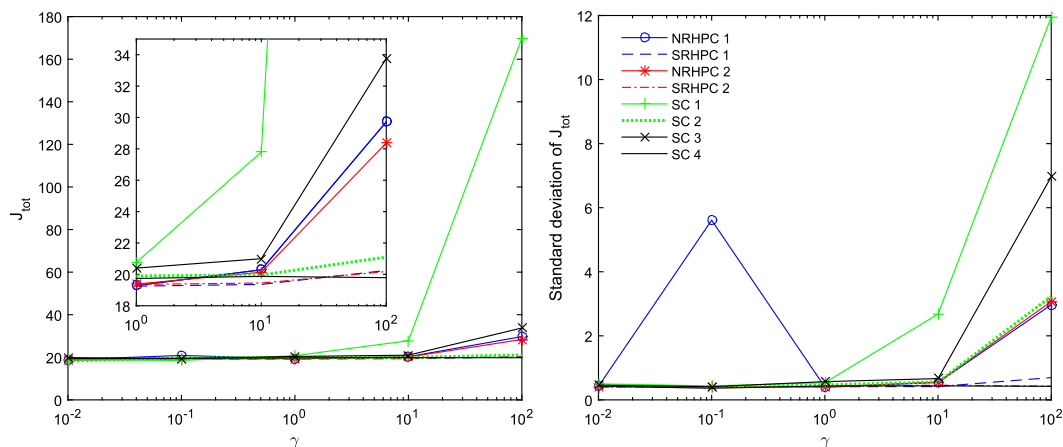


Figure 9. Total performance, Case 2 (with  $J_{tot}$  zoomed in for  $\gamma \in \{1, 10, 100\}$ ).

However, NRHPC 1 leads to higher queue length constraint violations (5.5%–25.5%) than SRHPC 1 (1.6%–13.4%) for all values of  $\gamma$  considered. For SRHPC 1, the queue length constraint violations (1.6%–2.3%) are relatively small when  $\gamma \in \{0.1, 1, 10, 100\}$ . Comparing the values of  $J_{tot}$ , we find that SRHPC 1 (15.9–17.3) results in better total performance than NRHPC 1 (16.3–21.2) for  $\gamma \in \{10, 100\}$ . For both NRHPC 1 and SRHPC 1, the standard deviations of  $J_{imp}^{TTS}$  and  $J_{tot}$  are small, and the standard deviations of  $J_{pen}$  are large.

The results for Case 2 are shown in Table II. Just as for Case 1, the performance improvements for SRHPC 1 (4.1%–4.7%) are less than the performance improvements for NRHPC 1 (4.4%–6.1%). For NRHPC 1, the queue length constraint violations (10.6%–53.4%, higher than for Case 1) are higher than those for SRHPC 1 (1.0%–18.2%) for all values of  $\gamma$  considered. For SRHPC 1, the queue length constraint violations (1.0%–2.5%) are relatively small when  $\gamma \in \{0.1, 1, 10, 100\}$ ; furthermore, for these values of  $\gamma$ , the total performance for SRHPC 1 (19.2–20.3) is not worse than the total performance for NRHPC 1 (19.3–29.7). The standard deviations of  $J_{imp}^{TTS}$  and  $J_{tot}$  are small for both NRHPC 1 and SRHPC 1 except for NRHPC 1 with  $\gamma = 0.1$ . For both NRHPC 1 and SRHPC 1, the standard deviations of  $J_{pen}$  are large.

(2) Results for NRHPC 2 and SRHPC 2:

The results for Case 1 are shown in Table III. The performance improvements for SRHPC 2 (5.0%–9.4%) are slightly less than the performance improvements for NRHPC 2 (5.1%–9.5%) when  $\gamma \in \{0.01, 0.1, 1\}$ . SRHPC 2 (5.2%) can even improve the performance more than NRHPC 2 (5.0%–5.1%) when  $\gamma \in \{10, 100\}$ . The queue length constraint violations for NRHPC 2 (3.0%–70.0%) are higher than those for SRHPC 2 (0.6%–66.3%) for all the values of  $\gamma$  considered. For  $\gamma \in \{0.1, 1, 10, 100\}$ , the queue length constraint violations for SRHPC 2 (0.6%–0.8%) are quite small. SRHPC 2 (16.0–16.4) results in a better total performance than NRHPC 2 (16.2–19.7) when  $\gamma \in \{10, 100\}$ . For both NRHPC 1 and SRHPC 1, the standard deviations of  $J_{imp}^{TTS}$  and  $J_{tot}$  are small, and the standard deviations of  $J_{pen}$  are large.

The results for Case 2 are shown in Table IV. For all the values of  $\gamma$  considered, the performance improvements for SRHPC 2 (3.7%–6.3%) are less than the performance improvements for NRHPC 2 (4.0%–7.2%). However, NRHPC 2 leads to higher queue length constraint violations (9.1%–125.7%, higher than for Case 1) than SRHPC 2 (0.8%–82.0%) for all values of  $\gamma$  considered. When  $\gamma \in \{0.1, 1, 10, 100\}$ , SRHPC 2 can reduce the queue length constraint violations (0.8%–2.7%) to relatively low values; furthermore, for these values of  $\gamma$ , the total performance for SRHPC 2 (19.3–20.2) is not worse than the total performance for NRHPC 2 (19.3–28.4). For both NRHPC 1 and SRHPC 1, the standard deviations of  $J_{imp}^{TTS}$  and  $J_{tot}$  are small, and the standard deviations of  $J_{pen}$  are large.

## (3) Results for SC 1 and SC 2:

The results for Case 1 are shown in Table V. For SC 1 with all values of  $\gamma$  considered and for SC 2 with  $\gamma \in \{0.01, 0.1\}$ , the performance improvements are 2.2%–12.1%, however, the queue length constraint violations (52.9%–114.2%) are quite high. For SC 2 with  $\gamma \in \{1, 10, 100\}$ , the queue length constraint violations (0%–0.1%) are small, and the performance improvements (1.6%–2.2%) are also small. For all the values of  $\gamma$  considered, the total performance for SC 2 (14.7–16.4) is better than the total performance for SC 1 (14.8–85.6). For SC 1, the standard deviations of  $J_{\text{imp}}^{\text{TTS}}$  and  $J_{\text{pen}}$  are large in general, and the standard deviations of  $J_{\text{tot}}$  are small except for  $\gamma = 0.01$ . For SC 2, the standard deviations of  $J_{\text{imp}}^{\text{TTS}}$ ,  $J_{\text{pen}}$ , and  $J_{\text{tot}}$  are small except for the standard deviations of  $J_{\text{pen}}$  with  $\gamma = 100$ .

The results for Case 2 are shown in Table VI. For SC 1 with all values of  $\gamma$  considered and for SC 2 with  $\gamma = 0.01$ , the performance improvements are 1.9%–9.3%, with high queue length constraint violations (82.1%–241.0%, higher than for Case 1). When  $\gamma \in \{0.1, 1, 10, 100\}$ , the queue length constraint violations are reduced to 0%–1.3% for SC 2, but the performance improvements are quite small (0.4%–1.3%). For  $\gamma \in \{1, 10, 100\}$ , the total performance for SC 2 (19.9–21.1) is better than the total performance for SC 1 (20.8–169.9). For SC 1 and SC 2, the standard deviations of  $J_{\text{imp}}^{\text{TTS}}$  and  $J_{\text{pen}}$  are large in general, and the standard deviations of  $J_{\text{tot}}$  are small in general.

## (4) Results for SC 3 and SC 4:

The results for Case 1 are shown in Table VII. For SC 3 with all values of  $\gamma$  considered and for SC 4 with  $\gamma \in \{0.01, 0.1\}$ , the performance is changed by –1.9%–4.6%, but the queue length constraint violations (6.6%–14.1%) are still high, even they are reduced w.r.t. SC 1 without queue override scheme. This is because when the mainstream is congested the vehicles at the on-ramp cannot enter the main road even if the ramp metering rate is 1. For SC 4 with  $\gamma \in \{1, 10, 100\}$ , the queue length constraint violations (0%–0.6%) are small, while the performance improvements (0.7%–2.8%) are also small. For SC 3 and SC 4, the standard deviations of  $J_{\text{imp}}^{\text{TTS}}$  and  $J_{\text{pen}}$  are large in general, and the standard deviations of  $J_{\text{tot}}$  are small in general.

The results for Case 2 are shown in Table VIII. For SC 3 with all values of  $\gamma$  considered and for SC 4 with  $\gamma \in \{0.01, 0.1\}$ , the performance is changed by –1.2%–3.8%, with high queue length constraint violations (8.3%–27.7%, higher than those for Case 1), which are reduced w.r.t. SC 1 without queue override scheme. For SC 4 with  $\gamma \in \{1, 10, 100\}$ , the queue length constraint violations are reduced to 0%–0.4%. Nevertheless, the performance improvements (1.0%–1.8%) are also small. For SC 3 and SC 4, the standard deviations of  $J_{\text{imp}}^{\text{TTS}}$  and  $J_{\text{pen}}$  are large in general, and the standard deviations of  $J_{\text{tot}}$  are small in general.

## (5) Overall comparison for all approaches:

The performance improvements for TTS ( $J_{\text{imp}}^{\text{TTS}}$ ), constraint violations ( $J_{\text{pen}}$ ), and total performance ( $J_{\text{tot}}$ ) for all approaches considered are plotted in Figures 4–9. In these figures, the lines with marker symbols correspond to the approaches ignoring uncertainties (NRHPC 1, NRHPC 2, SC 1, and SC 3), and the lines without marker symbols correspond to the approaches including uncertainties (SRHPC 1, SRHPC 2, SC 2, and SC 4).

For both cases of uncertainties (Case 1 and Case 2), the performance improvements for TTS for SC 2, SC 3, and SC 4 are small in comparison with NRHPC 1, NRHPC 2, SRHPC 1, and SRHPC 2 when  $\gamma \in \{1, 10, 100\}$ . For SC 1, the queue length constraint violations are much higher than those for NRHPC 1 and NRHPC 2 for both cases of uncertainties (Case 1 and Case 2). Including a queue override scheme, the queue length constraint violations for SC 3 are comparable with those for NRHPC 1 and NRHPC 2 for both cases of uncertainties (Case 1 and Case 2). The queue length constraint violations are reduced to low values for SRHPC 1, SRHPC 2, SC 2, and SC 4 when the weight  $\gamma$  for the queue length penalty is large enough, for example,  $\gamma \in \{1, 10, 100\}$ . In  $J_{\text{tot}}$ , a larger weight  $\gamma$  for the queue length penalty corresponds

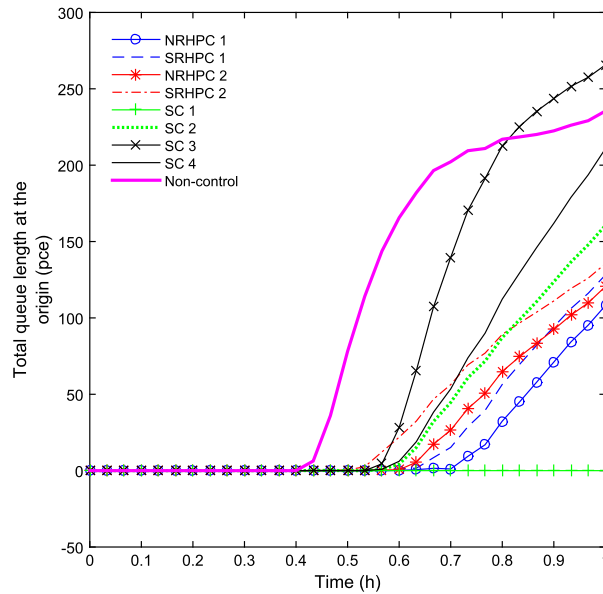


Figure 10. Queue lengths at the origin, Case 1.

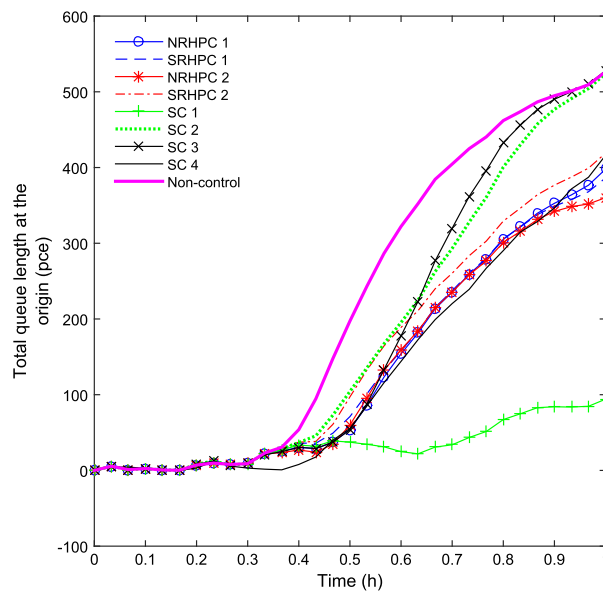


Figure 11. Queue lengths at the origin, Case 2.

to assigning more importance to satisfying the queue length constraint. When the weight  $\gamma$  is large enough (e.g.,  $\gamma \in \{10, 100\}$ ), the total performance for SRHPC 1, SRHPC 2, SC 2, and SC 4 is better than NRHPC 1, NRHPC 2, SC 1, and SC 3.

**4.3.2. Analysis for queue lengths and control inputs.** Here, one realization for Case 1 of uncertainties and one realization for Case 2 of uncertainties are chosen as examples. The queue lengths for the origin, the queue lengths for the on-ramp, variable speed limits, and ramp metering rates for all the considered control approaches with  $\gamma = 100$  are respectively shown in Figures 10–17. The plots of other traffic variables (origin flows, on-ramp flows, flows for segments, speeds for segments, and densities for segments) that are used for describing the traffic network are included and discussed in Appendix A.

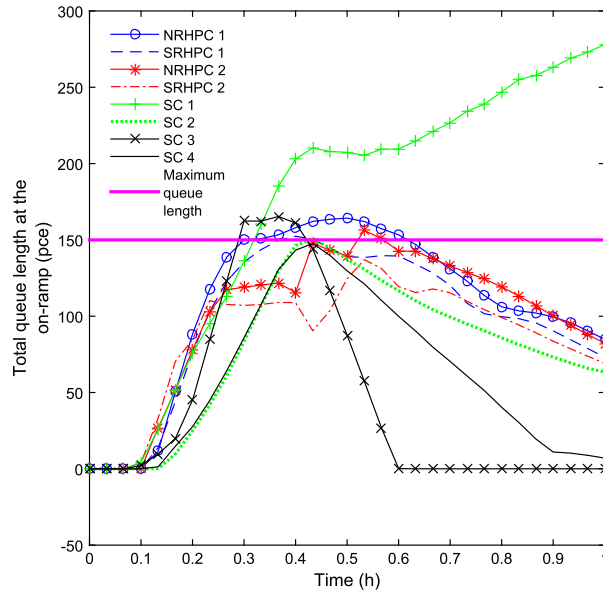


Figure 12. Queue lengths at the on-ramp, Case 1.

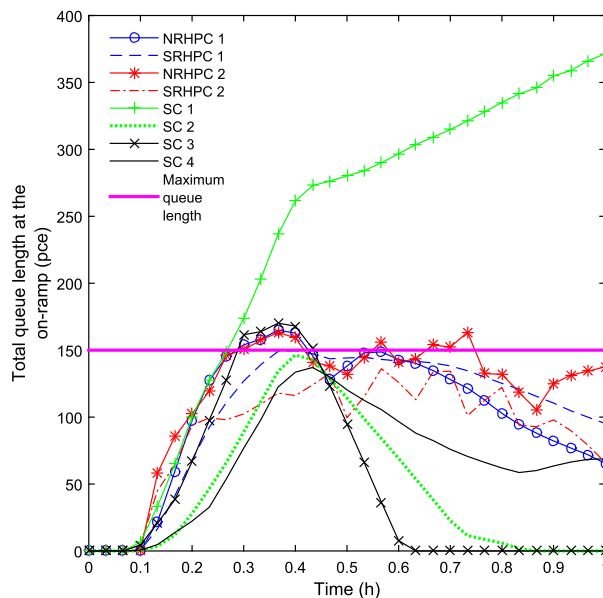


Figure 13. Queue lengths at the on-ramp, Case 2.

According to Figures 10–11, the queue lengths at the origin are decreased in comparison with the non-control cases for both the nominal RHPC approaches (NRHPC 1 and NRHPC 2) and the scenario-based RHPC approaches (SRHPC 1 and SRHPC 2). For standard control approaches (SC 1, SC 2, and SC 4), the queue lengths at the origin can also be reduced, except for SC 3 from  $t = 0.8$  h on.

According to Figures 12–13, the control approaches ignoring uncertainties (NRHPC 1, NRHPC 2, SC1, and SC 3) lead to queue length constraint violations. These queue length constraint violations are effectively reduced by the control approaches considering uncertainties (SRHPC 1, SRHPC 2, SC 2, and SC 4).

As shown in Figures 14 and 16, the variable speed limits of the nominal RHPC approaches (NRHPC 1 and NRHPC 2) are similar with those of the scenario-based RHPC approaches (SRHPC

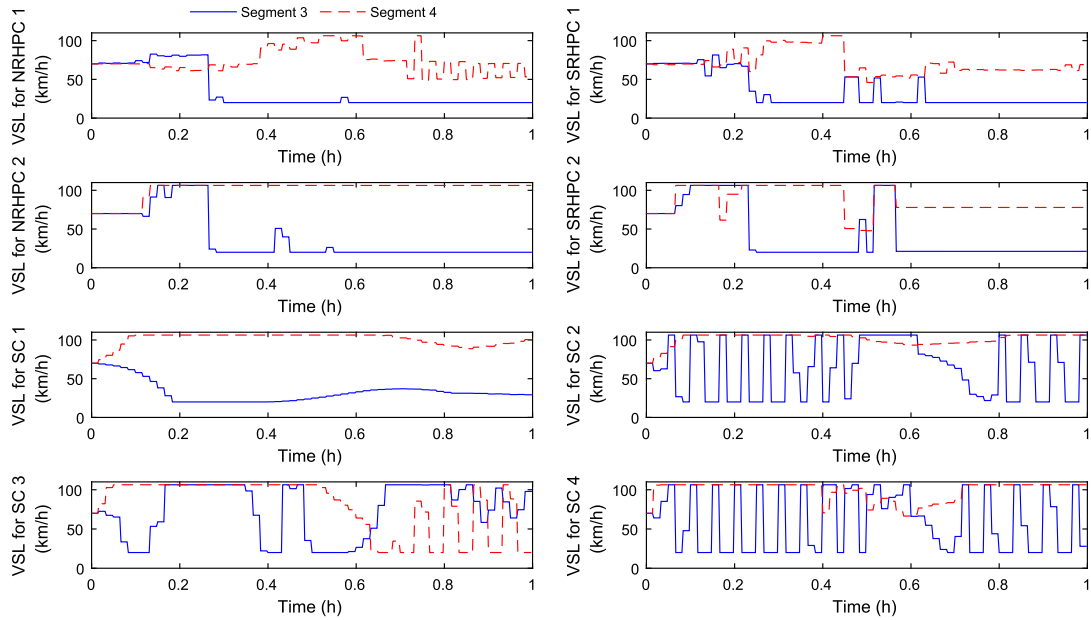


Figure 14. Variable speed limits, Case 1.

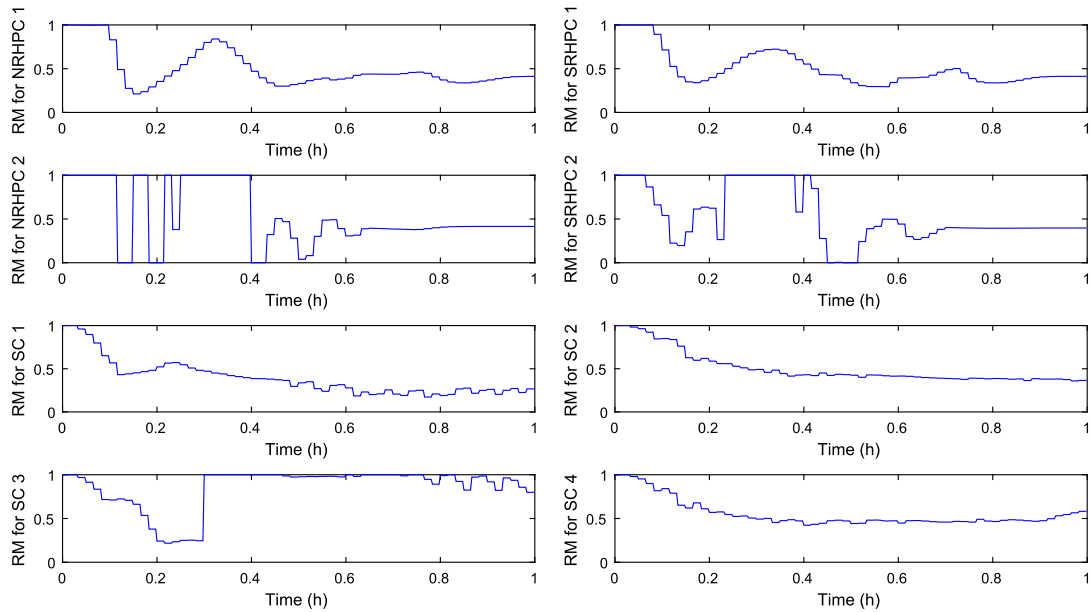


Figure 15. Ramp metering rates, Case 1.

1 and SRHPC 2), and there are no large fluctuations for both of them. However, the standard control approaches (SC 2, SC 3, and SC 4) except SC 1 yield variable speed limits that fluctuate more than the nominal RHPC approaches (NRHPC 1 and NRHPC 2) and the scenario-based RHPC approaches (SRHPC 1 and SRHPC 2).

Figures 15 and 17 show the ramp metering rates. The nominal RHPC approaches (NRHPC 1 and NRHPC 2) and the scenario-based RHPC approaches (SRHPC 1 and SRHPC 2) can appropriately address the variations in the demand for the on-ramp, that is, the ramp metering rates increase when there is a peak in the on-ramp demand from  $t = 0.1$  h to  $t = 0.35$  h (as shown in

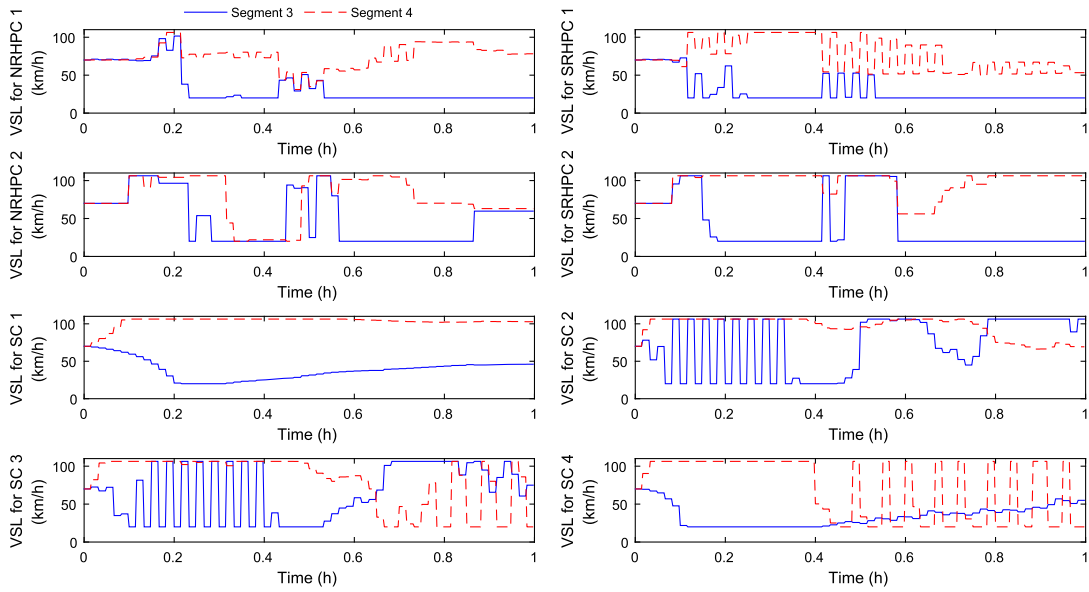


Figure 16. Variable speed limits, Case 2.

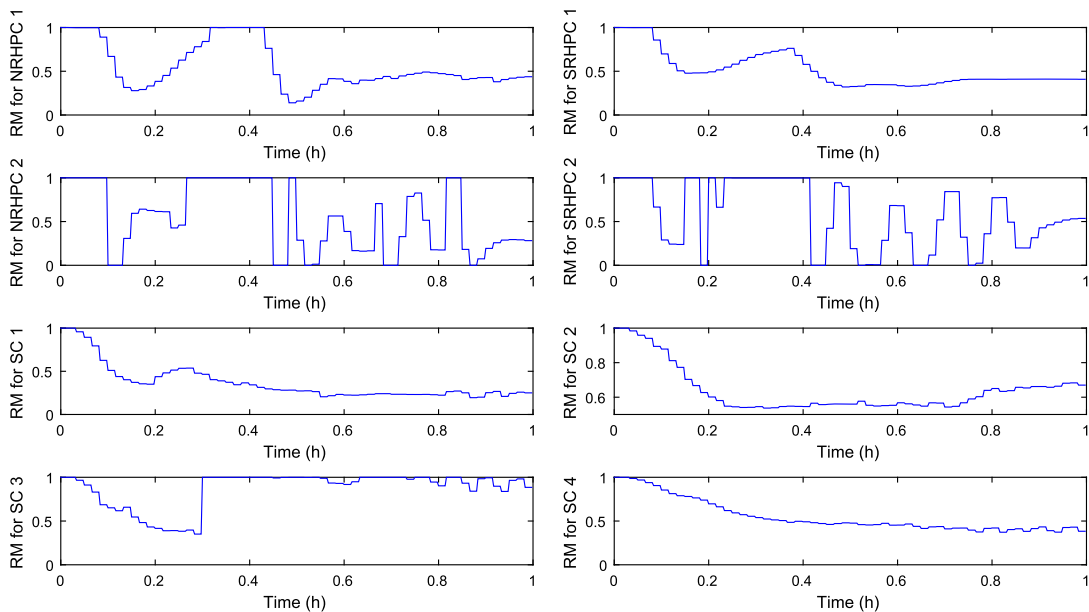


Figure 17. Ramp metering rates, Case 2.

Figure 3). However, for the standard control approaches, the ramp metering rates do not increase in a similar way.

4.3.3. *Conclusions of results.* According to the results of the previous approaches, we can give the following conclusions:

- (1) The nominal RHPC approaches ignoring uncertainties (NRHPC 1 and NRHPC 2) can improve the performance with high queue length constraint violations for all the considered values of the weight  $\gamma$  for the queue length penalty.
- (2) The scenario-based RHPC approaches including uncertainties (SRHPC 1 and SRHPC 2) can also improve the performance, while there may be a small sacrifice in the performance

- improvement compared with the nominal RHPC approaches ignoring uncertainties (NRHPC 1 and NRHPC 2). The queue length constraint violations are significantly reduced w.r.t. the nominal RHPC approaches ignoring uncertainties (NRHPC 1 and NRHPC 2) when the weight  $\gamma$  for the queue length penalty is large enough.
- (3) The scenario-based RHPC approaches including uncertainties (SRHPC 1 and SRHPC 2) are more conservative in improving performance and satisfying the queue length constraints than the nominal RHPC approaches ignoring uncertainties (NRHPC 1 and NRHPC 2). This may be because the scenario-based RHPC approaches including uncertainties (SRHPC 1 and SRHPC 2) are optimizing the worst case among all the considered scenarios.
  - (4) The standard control approach ignoring uncertainties (SC 1) can improve the control performance; however, the queue length constraint violations are quite high for all the considered values of the weight  $\gamma$  for the queue length penalty. Even when a queue override scheme is included in the standard control approach ignoring uncertainties (SC 3), there are still high constraint violations. This is because when the mainstream is congested, the vehicles at the on-ramp cannot enter the main road even if the ramp metering rate is 1.
  - (5) The standard control approaches including uncertainties (SC 2 and SC 4) can significantly reduce the queue length constraint violations when the weight  $\gamma$  for the queue length penalty is large enough. However, the performance improvements for these approaches are less than those for the scenario-based RHPC approaches including uncertainties (SRHPC 1 and SRHPC 2).
  - (6) When there are also uncertainties in the truck fractions (Case 2), the queue length constraint violations may be even higher in comparison with the case that there are only uncertainties in the total demand (Case 1).
  - (7) There are still small queue length constraint violations for the approaches including uncertainties (SRHPC 1, SRHPC 2, SC 2, and SC 4). This is probably because we use only a limited number of scenarios for the uncertainties when solving the control problem.
  - (8) When the weight  $\gamma$  for the queue length penalty is large enough (in general,  $\gamma = 1$  in our case study) for the approaches including uncertainties (SRHPC 1, SRHPC 2, SC 2, and SC 4), the queue length constraint violations are reduced significantly. Increasing this weight  $\gamma$  to be even larger ( $\gamma \in \{10, 100\}$ ) does not significantly affect the performance improvements and the ability of reducing queue length constraint violations. However, a larger weight  $\gamma$  for the queue length penalty corresponds to putting more emphasis on satisfying the queue length constraint. When the weight  $\gamma$  is large enough (e.g.,  $\gamma \in \{10, 100\}$ ), the total performance for the approaches including uncertainties (SRHPC 1, SRHPC 2, SC 2, and SC 4) is better than that for the approaches ignoring uncertainties (NRHPC 1, NRHPC 2, SC 1, and SC 3).
  - (9) According to standard deviations, the RHPC approaches (NRHPC 1, NRHPC 2, SRHPC 1, and SRHPC 2) are comparable in the performance improvement for different scenarios considered, but they differ in the queue length constraint violations for different scenarios considered. Note that for the scenario-based RHPC approaches (SRHPC 1 and SRHPC 2), the queue length constraint violations are minor when the weight  $\gamma$  for the queue length penalty is large enough; although the relative standard deviations are large, the actual variations in these violations are still small. The standard control approaches SC 1, SC 3, and SC 4 differ in both the performance improvement and the queue length constraint violations for the different scenarios considered.
  - (10) The variable speed limits of the standard control approaches SC 2, SC 3, and SC 4 fluctuate more than those of the RHPC approaches (NRHPC 1, NRHPC 2, SRHPC 1, and SRHPC 2). The RHPC approaches (NRHPC 1, NRHPC 2, SRHPC 1, and SRHPC 2) can appropriately address the peak in the on-ramp demand by increasing the ramp metering rates at corresponding time; however, the standard control approaches (SC 1, SC 2, SC 3, and SC 4) do not increase the ramp metering rates in a similar way.

In conclusion, we can say that the scenario-based RHPC approaches are effective for satisfying the queue length constraint, at the cost of a small sacrifice in performance. Avoiding high queue length constraint violations is significant for those on-ramps with strict limits on queue lengths,

for example, the on-ramps that are connected to busy urban stretches or intersections in upstream. High queue length constraint violations at these on-ramps may cause spillback to upstream; thus, scenario-based RHPC approaches are helpful for these on-ramps.

## 5. CONCLUSIONS AND FUTURE WORK

In this paper, we have developed a tractable scenario-based RHPC approach for freeway networks. In this approach, the worst-case scenario among a selected number of scenarios for uncertainties is considered in the control design step. On the basis of traffic states, we have developed several RHPC laws for freeway networks based on the multi-class METANET model. In addition, a soft queue length constraint penalty is included in the objective function instead of hard constraint, to prevent infeasible optimization problems under uncertainties. In the analysis of the uncertainties for freeway networks we in particular consider uncertainties in the demand profiles, consisting of the uncertainties in the total demand and the uncertainties in the estimations of the fractions of different classes of vehicles. However, other types of uncertainties can also be dealt with using the proposed scenario-based RHPC approach.

A case study was implemented to assess the effectiveness of this newly proposed approach. Two combinations of the RHPC laws for VSL and RM were considered: VSL law based on the variations in the speeds and densities from one segment to the next + ALINEA-like RM law and PI-ALINEA-like VSL law + PI-ALINEA-like RM law, for which both nominal RHPC approaches and scenario-based RHPC approaches were implemented. Standard control approaches (PI-ALINEA-like) were implemented for comparison, and a queue override scheme was also considered as extra comparison. The results show that the nominal RHPC approaches may lead to high queue length constraint violations even if the weight for the queue length penalty is high. The scenario-based RHPC approaches are more conservative than the nominal RHPC approaches, and they can significantly reduce the queue length constraint violations when the weight for the queue length penalty is high enough, with small sacrifices in performance improvements. The standard control approach ignoring uncertainties may lead to high queue length constraint violations, which are still high even when the queue override scheme is used. This is because when the mainstream is congested, the vehicles at the on-ramp cannot enter the main road even if the ramp metering rate is 1. The standard control approaches including uncertainties can reduce the queue length constraint violations to low level when the weight for the queue length penalty is large enough; however, the performance improvements are less than those for the scenario-based RHPC approaches. Overall, we can conclude that scenario-based RHPC is capable of significantly improving performance without high queue length constraint violations for the given case study.

For the future research, we will consider further extension of the RHPC laws for multi-class traffic networks, validation in real motorway with real data and larger freeway networks, theoretical guarantees for scenario-based RHPC, and the sensitivity to model parameters. In addition, it is hard to analyze analytically the stability and robustness for nonlinear systems, in-depth assessments using simulations for multiple setups and scenarios can be implemented in the future.

## APPENDIX: EXAMPLES FOR THE PLOTS OF TRAFFIC VARIABLES

For Case 1 and Case 2 of uncertainties, the same realizations as in Section 4.3.2 are chosen as examples. The origin flows, on-ramp flows, flows for segments, speeds for segments, and densities for segments for all the considered control approaches with  $\gamma = 100$  are respectively shown in Figures A.1–A.16.

The flows for the mainstream origin and the on-ramp are plotted in Figures A.1–A.4. We can see that the flows for the mainstream origin are similar for all the considered approaches except for SC 1. For different control approaches, the flows for the on-ramp correspond to ramp metering rates shown in Figures 15 and 17. The flows for segments are plotted in Figures A.5–A.8. As shown in these figures, the flows for the standard control approaches (SC 1, SC 2, SC 3, and SC 4) fluctuate more than those for the RHPC approaches (NRHPC 1, NRHPC 2, SRHPC 1, and SRHPC 2). The speeds

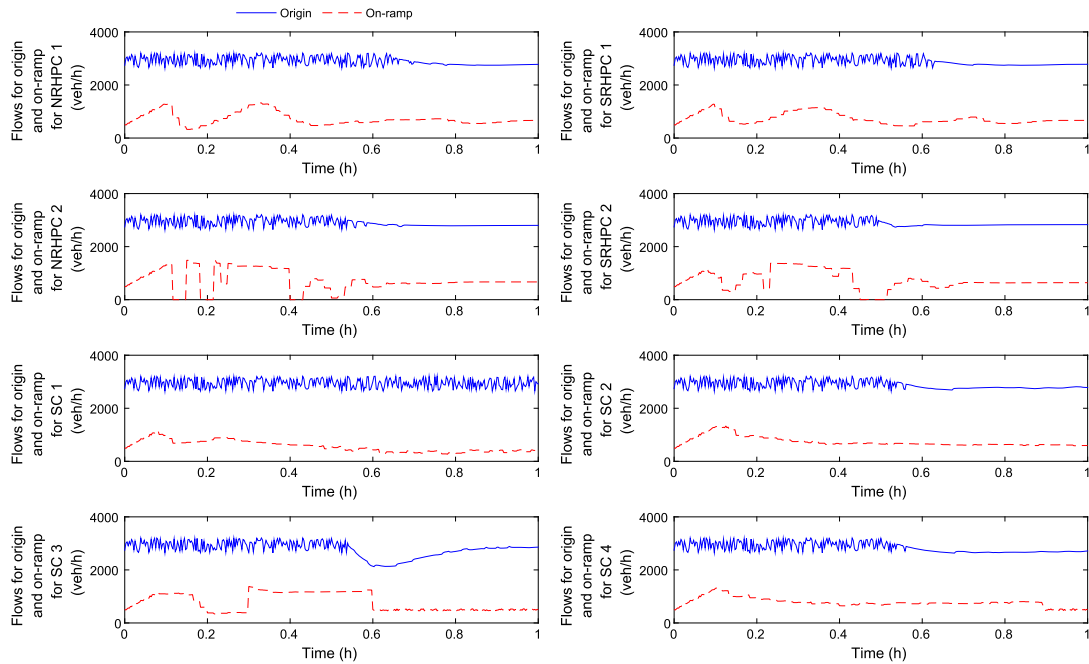


Figure A.1. Flows at the origin and the on-ramp for cars, Case 1.

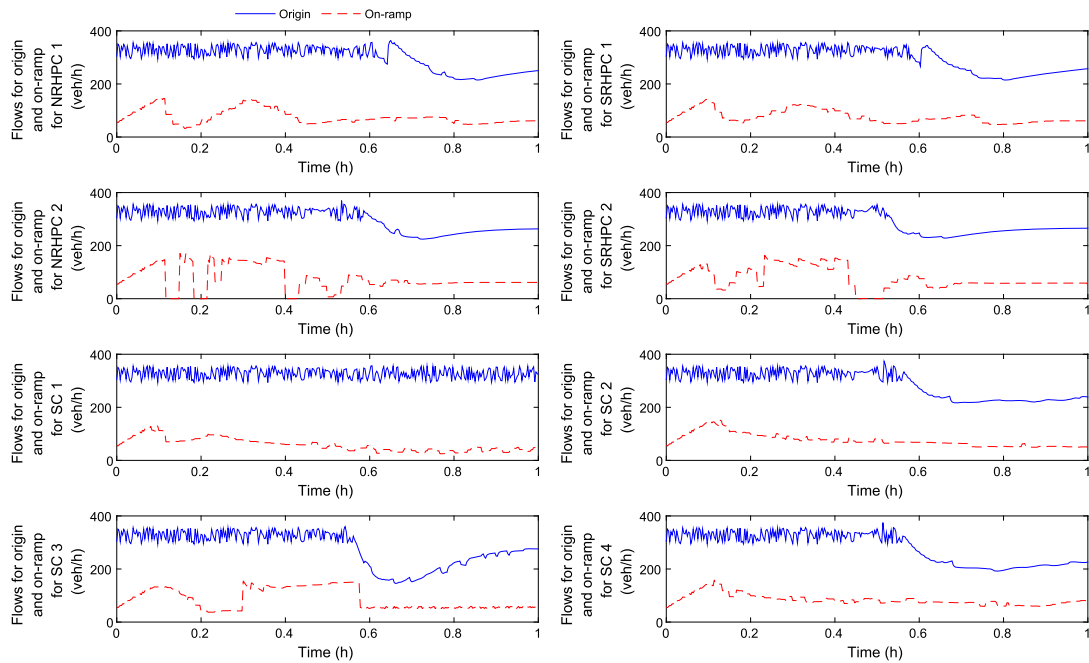


Figure A.2. Flows at the origin and the on-ramp for trucks, Case 1.

for segments are plotted in Figures A.9–A.12. The speeds for the standard control approaches (SC 1, SC 2, SC 3, and SC 4) fluctuate more than those for the RHPC approaches (NRHPC 1, NRHPC 2, SRHPC 1, and SRHPC 2). The fluctuations in the flows and speeds for segments correspond to variable speed limits shown in Figures 14 and 16. The densities for segments are plotted in Figures A.13–A.16. According to these figures, the evolution of the densities for segments is similar for all the considered approaches.

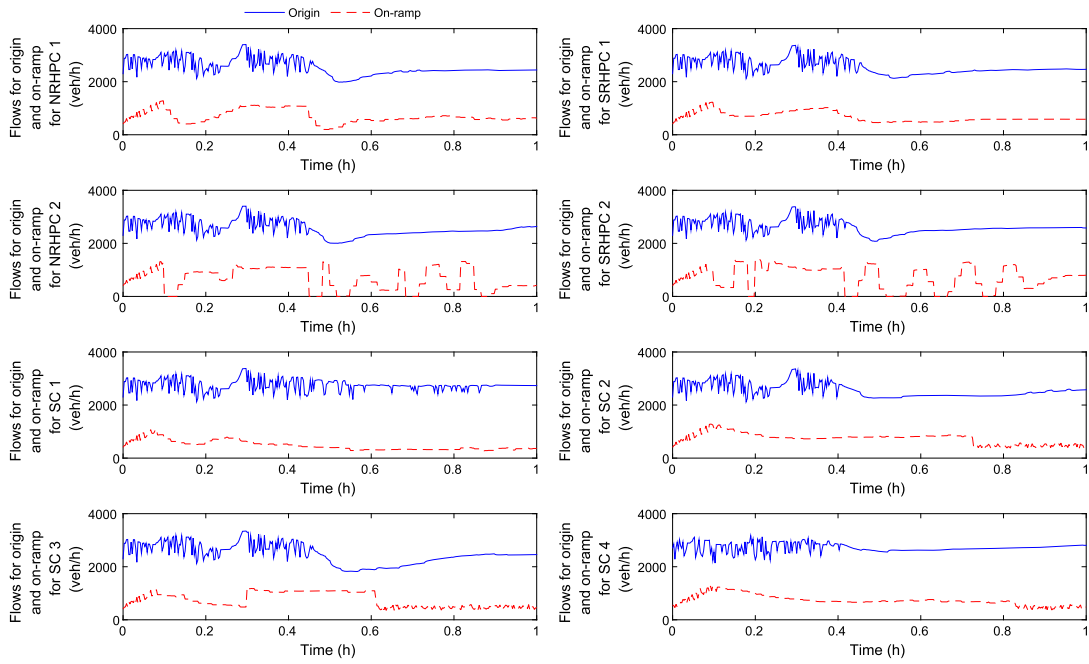


Figure A.3. Flows at the origin and the on-ramp for cars, Case 2.

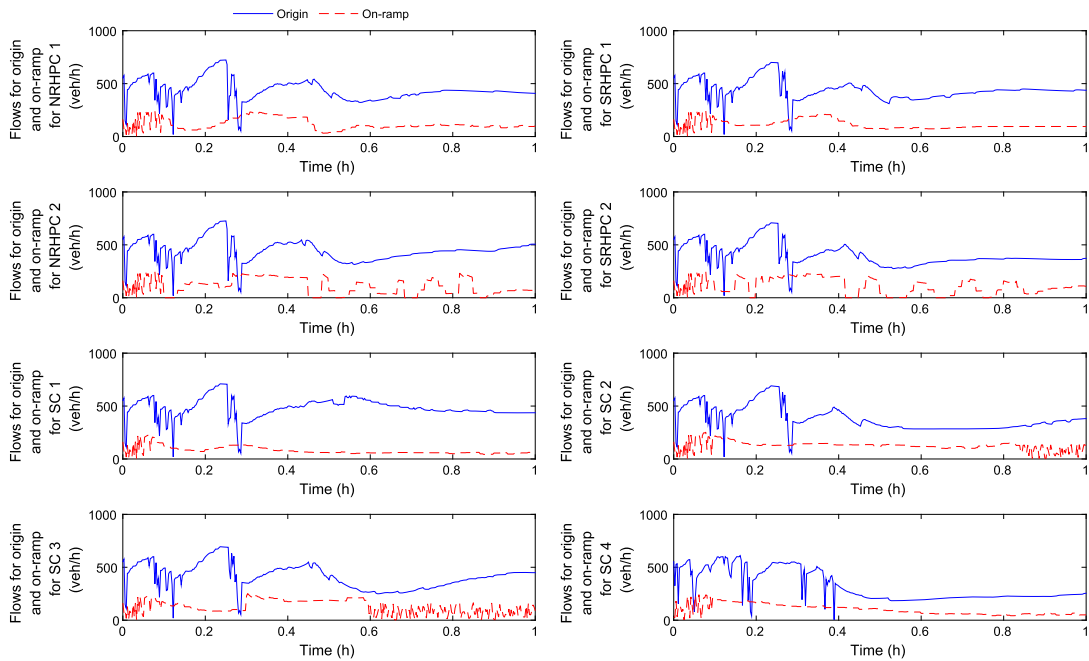


Figure A.4. Flows at the origin and the on-ramp for trucks, Case 2.

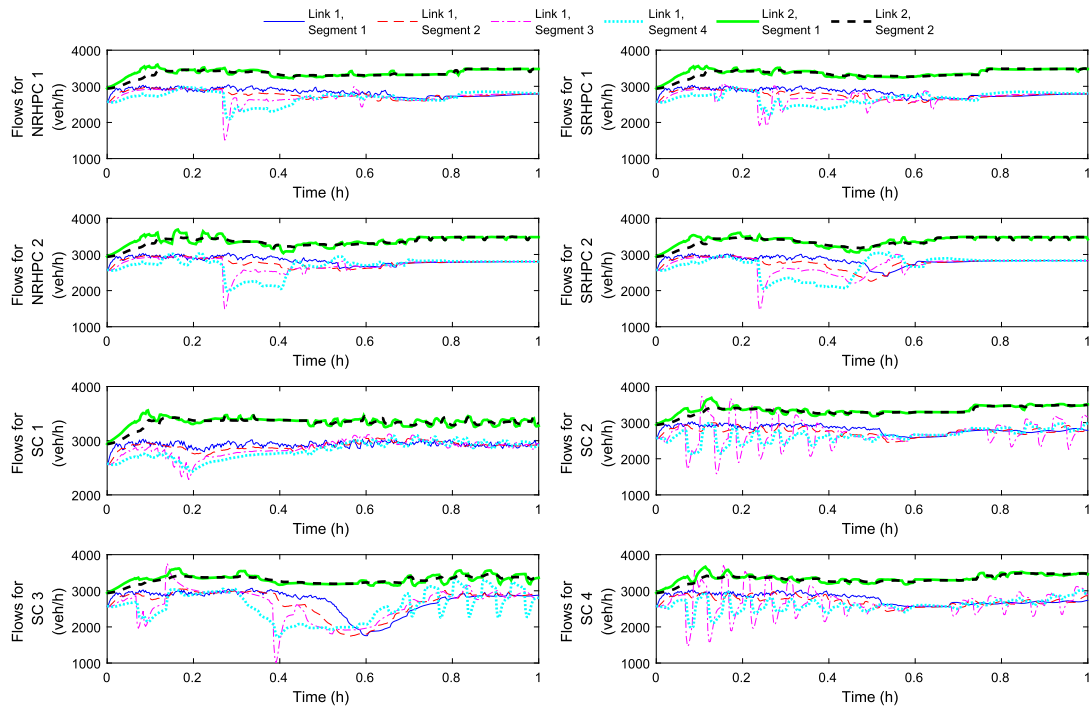


Figure A.5. Flows for segments, cars, Case 1.

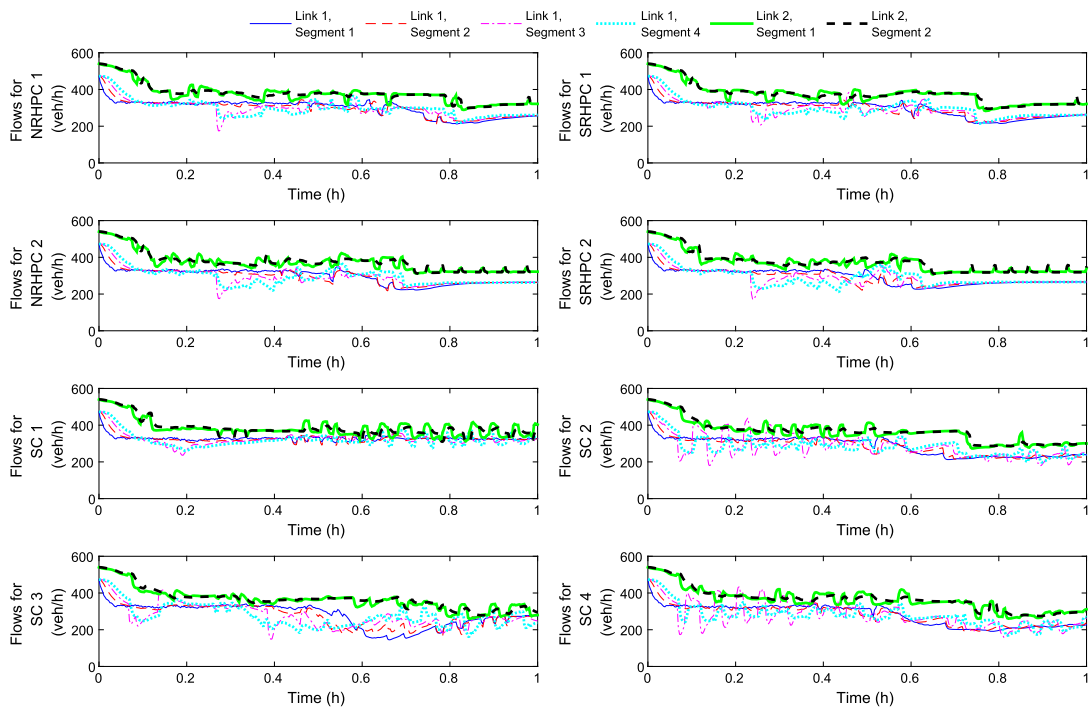


Figure A.6. Flows for segments, trucks, Case 1.

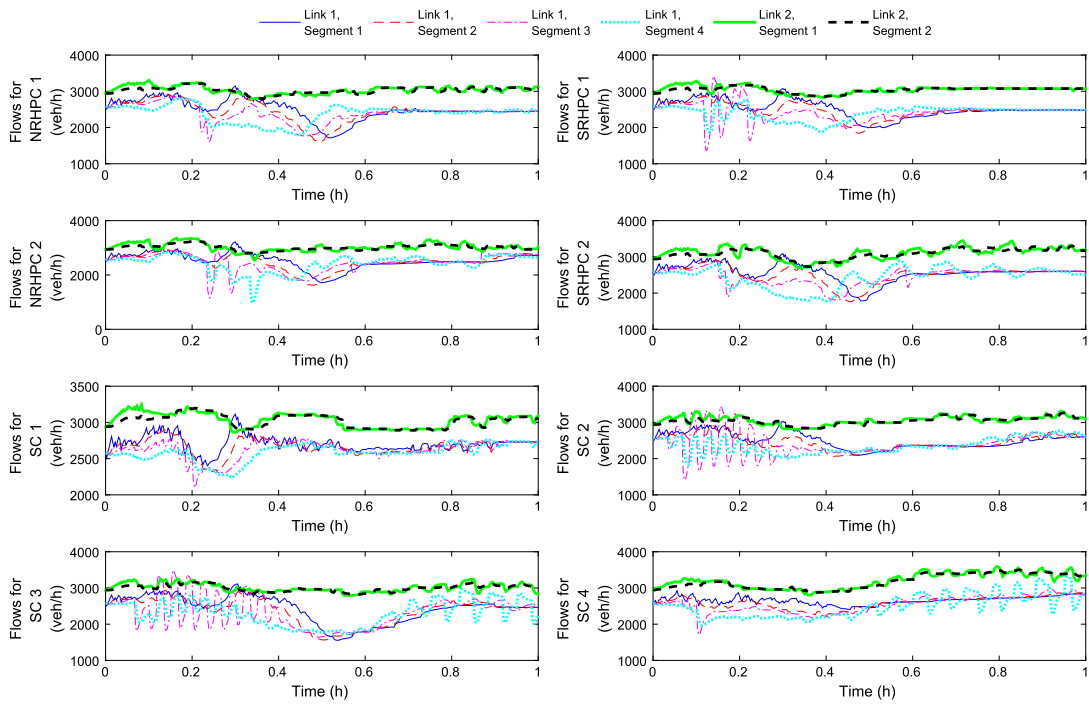


Figure A.7. Flows for segments, cars, Case 2.

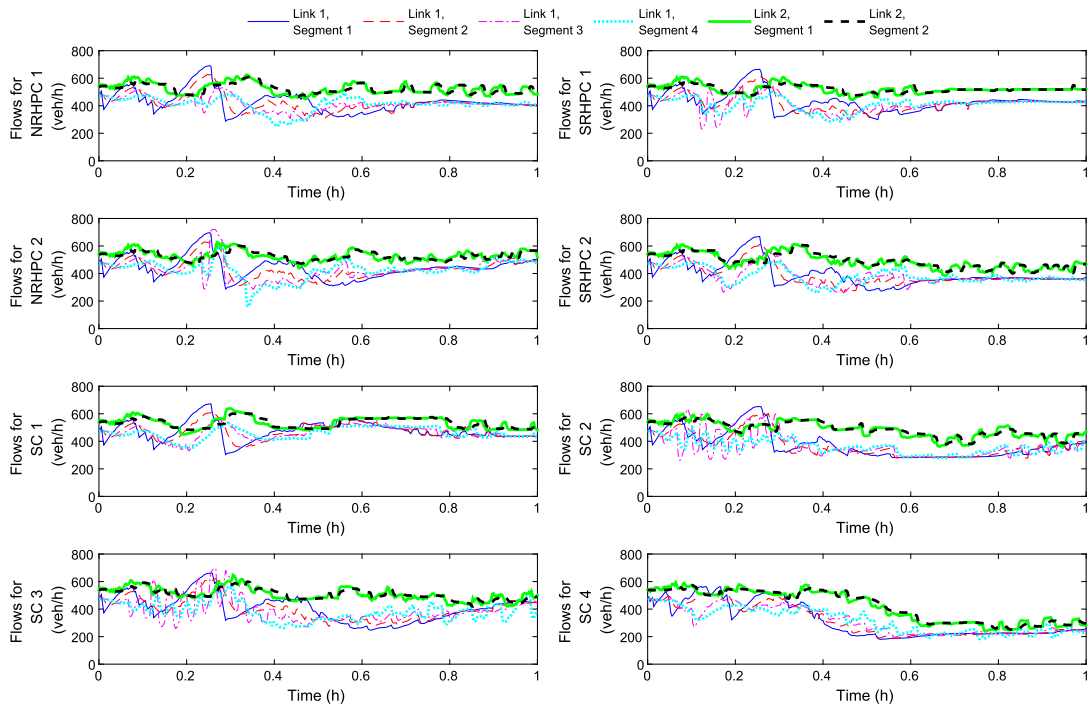


Figure A.8. Flows for segments, trucks, Case 2.

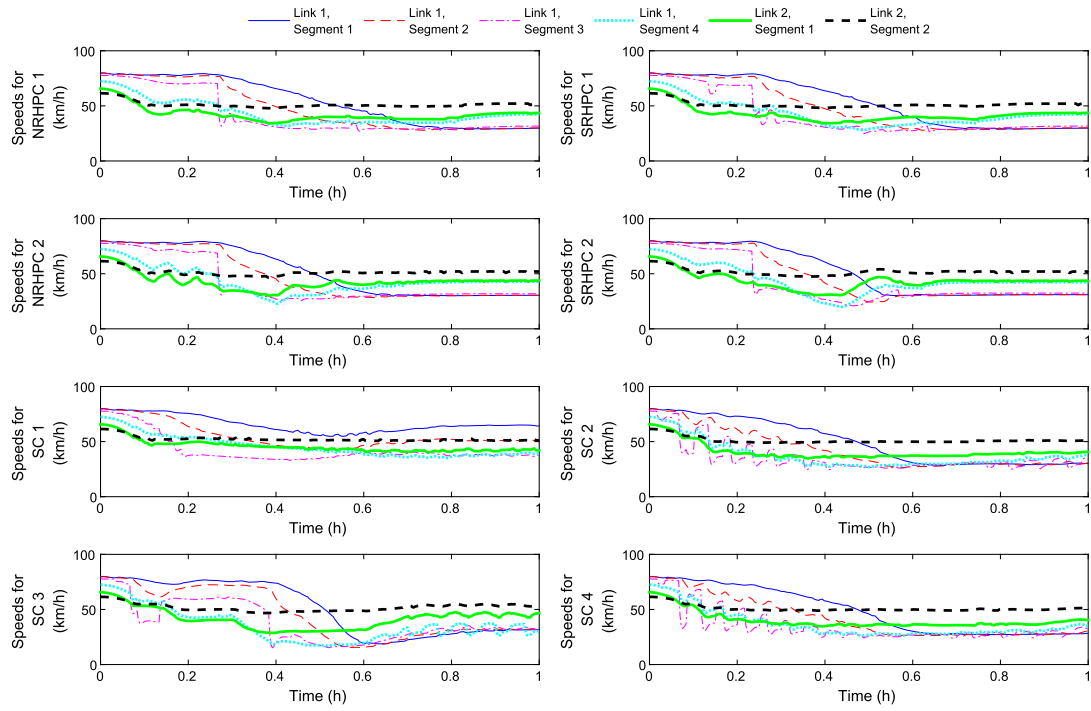


Figure A.9. Speeds for segments, cars, Case 1.

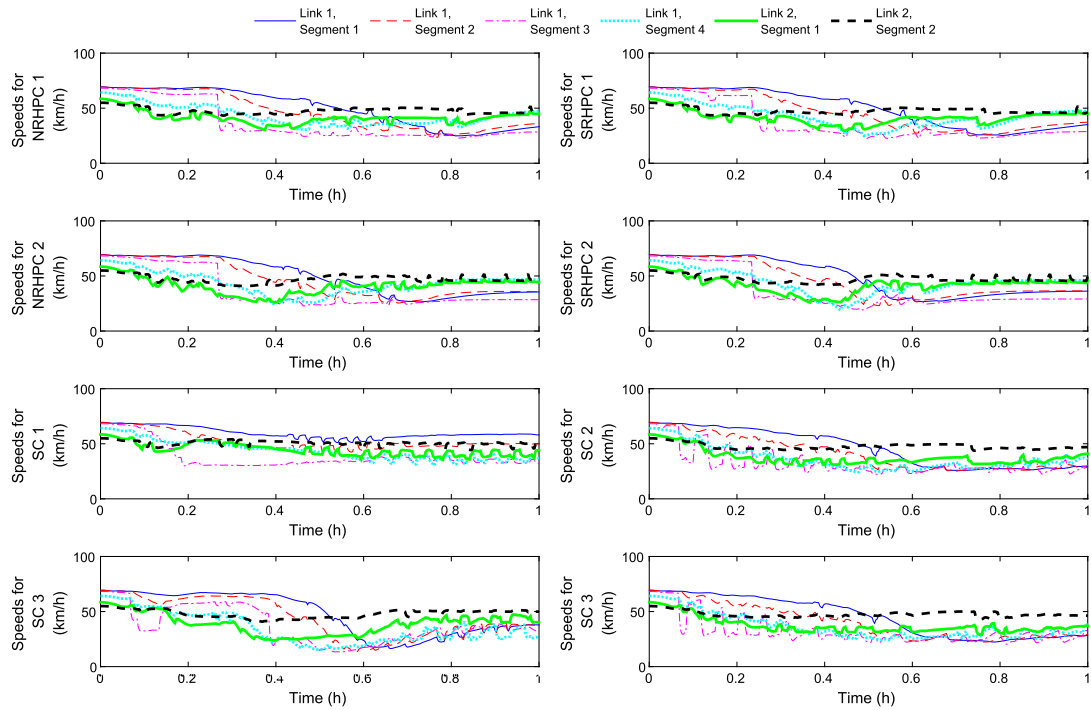


Figure A.10. Speeds for segments, trucks, Case 1.

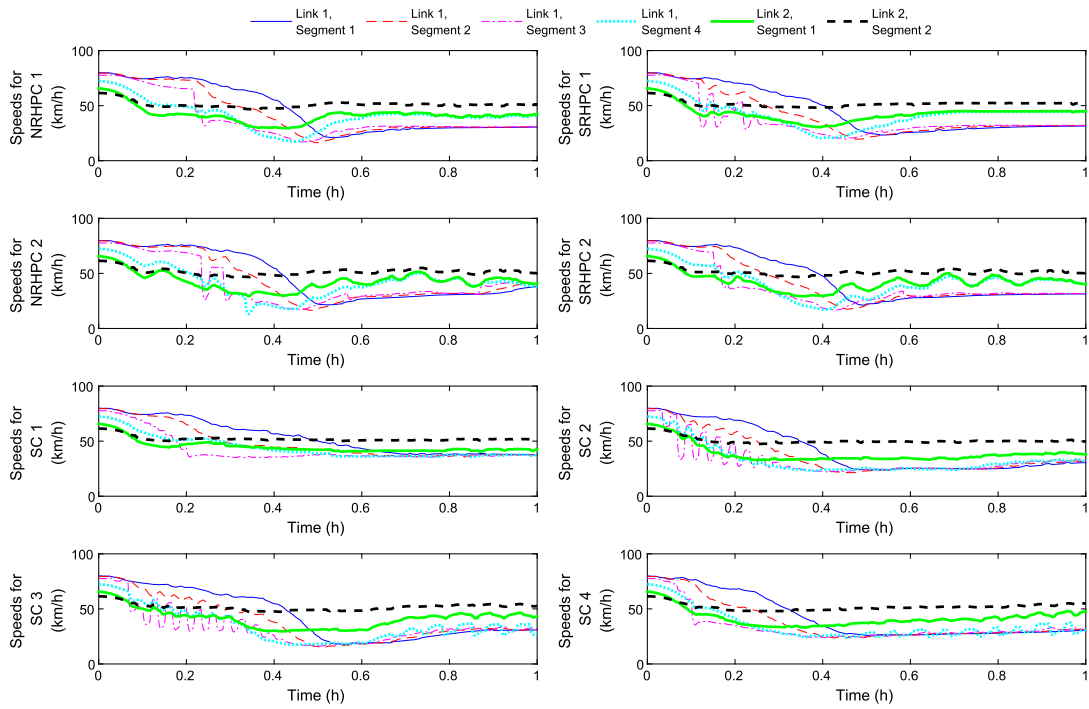


Figure A.11. Speeds for segments, cars, Case 2.

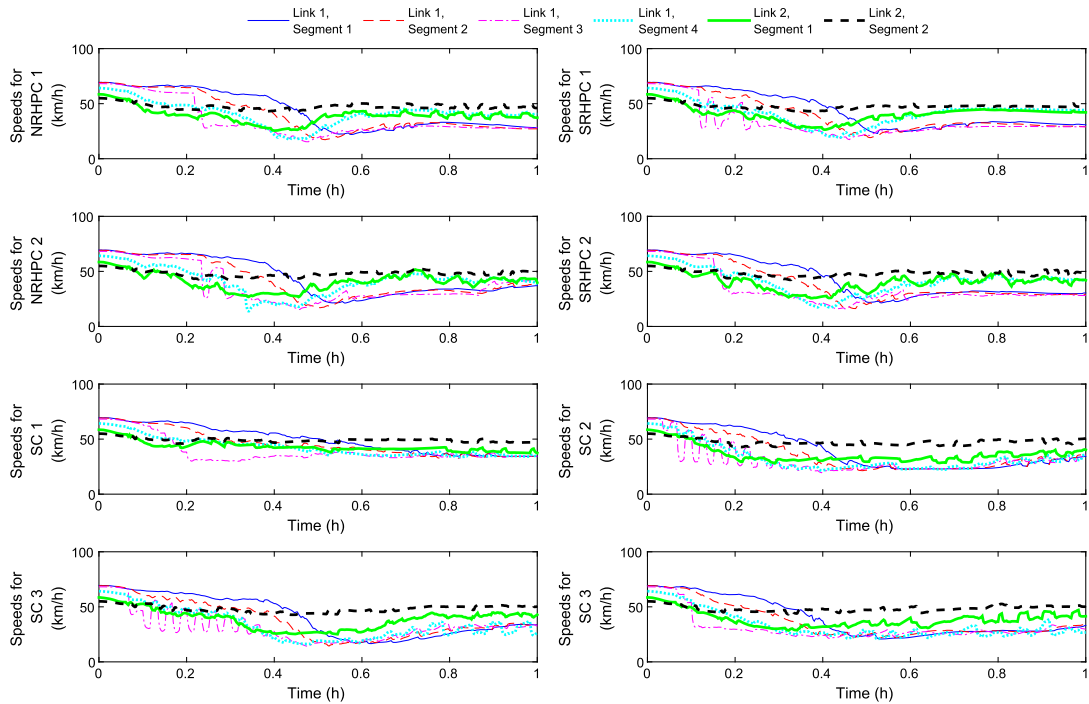


Figure A.12. Speeds for segments, trucks, Case 2.

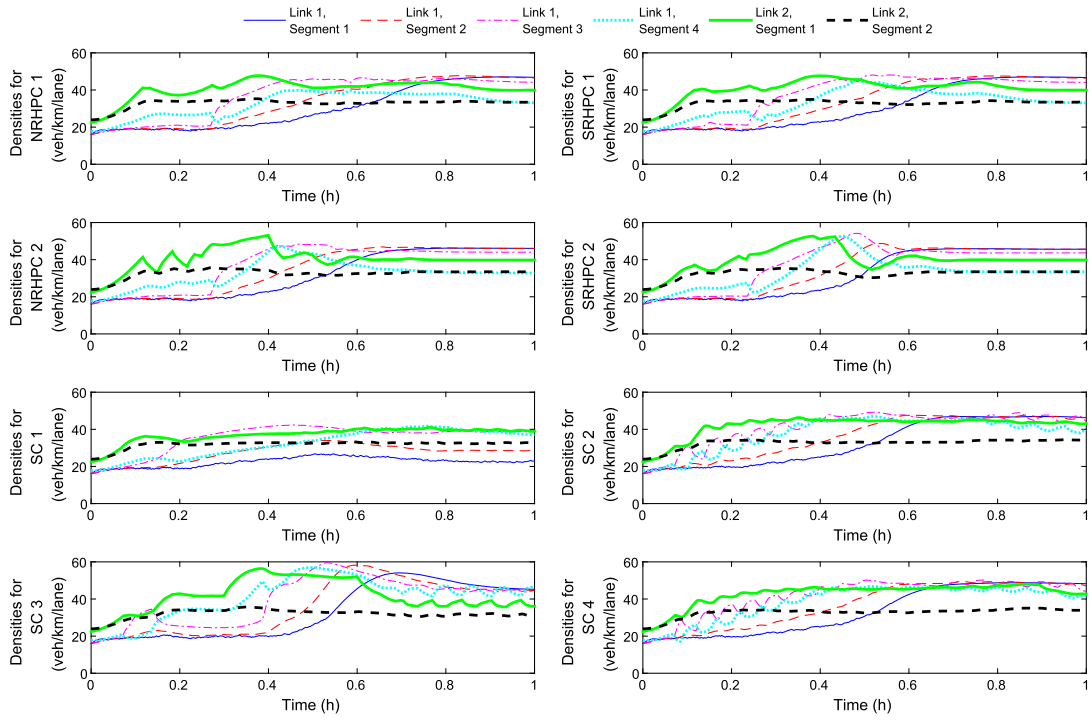


Figure A.13. Densities for segments, cars, Case 1.

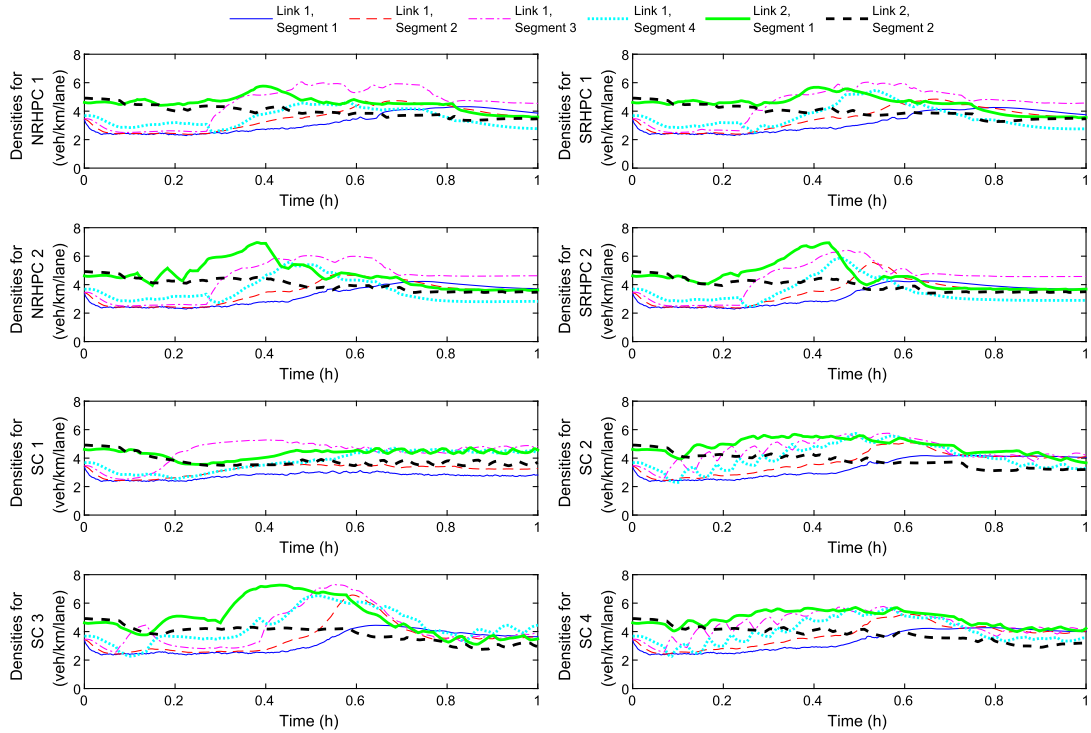


Figure A.14. Densities for segments, trucks, Case 1.

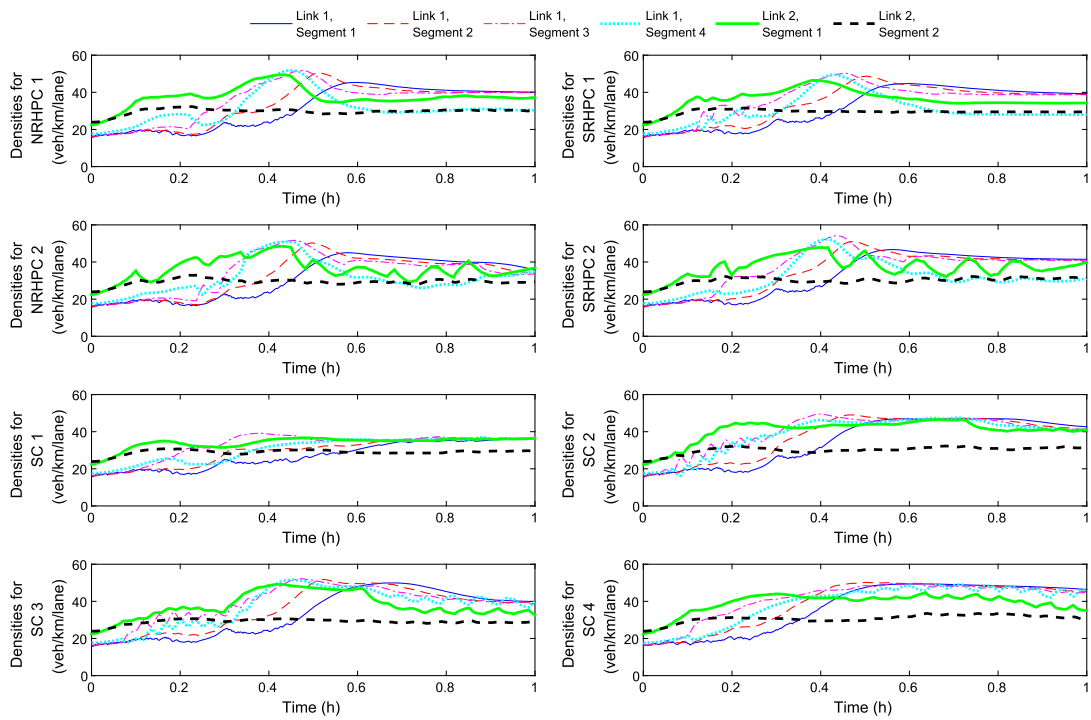


Figure A.15. Densities for segments, cars, Case 2.

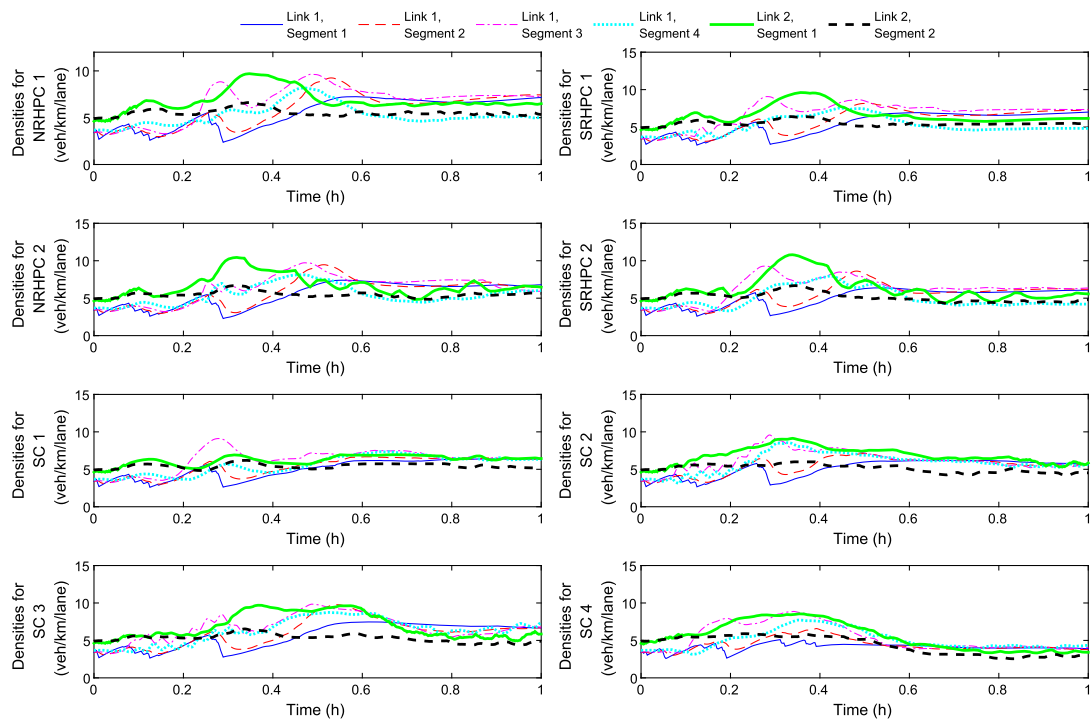


Figure A.16. Densities for segments, trucks, Case 2.

## ACKNOWLEDGEMENTS

This research is supported by the China Scholarship Council and the European COST Action TU1102.

## REFERENCES

1. Hegyi A, De Schutter B, Hellendoorn H. Model predictive control for optimal coordination of ramp metering and variable speed limits. *Transportation Research Part C: Emerging Technologies* 2005; **13**(3):185–209.
2. Caligaris C, Sacone S, Siri S. Multiclass freeway traffic: model predictive control and microscopic simulation. *Proceedings of 16th Mediterranean Conference on Control and Automation*, Ajaccio, France, 2008; 1862–1867.
3. Papamichail I, Kotsialos A, Margonis I, Papageorgiou M. Coordinated ramp metering for freeway networks—a model-predictive hierarchical control approach. *Transportation Research Part C: Emerging Technologies* 2010; **18**(3): 311–331.
4. Frejo JRD, Camacho EF. Global versus local MPC algorithms in freeway traffic control with ramp metering and variable speed limits. *IEEE Transactions on Intelligent Transportation Systems* 2012; **13**(4):1556–1565.
5. Wong GCK, Wong SC. A multi-class traffic flow model—an extension of LWR model with heterogeneous drivers. *Transportation Research Part A: Policy and Practice* 2002; **36**(9):827–841.
6. Schreiter T, Landman RL, van Lint JWC, Hegyi A, Hoogendoorn S. Vehicle class-specific route guidance of freeway traffic by model-predictive control. *Transportation Research Record* 2012; **2324**:53–62.
7. Liu S, De Schutter B, Hellendoorn J. Model predictive traffic control based on a new multi-class METANET model. *Proceedings of the 19th World Congress of the International Federation of Automatic Control*, Cape Town, South Africa, 2014; 8781–8786.
8. Liu S, Hellendoorn J, De Schutter B. Model predictive control for freeway networks based on multi-class traffic flow and emission models. *Technical Report 15–020*, Delft Center for Systems and Control, Delft University of Technology, Delft, The Netherlands, 2015. Submitted to a journal.
9. Scolaert POM, Rawlings JB, Meadows ES. Discrete-time stability with perturbations: application to model predictive control. *Automatica* 1997; **33**(3):463–470.
10. De Nicolao G, Magni L, Scattolini R. Stabilizing receding-horizon control of non-linear time-varying systems. *IEEE Transactions on Automatic Control* 1998; **43**(7):1030–1036.
11. Campo PJ, Morari M. Robust model predictive control. *Proceedings of the American Control Conference*, Minneapolis, USA, 1987; 1021–1026.
12. Gruber JK, Ramírez DR, Limon D, Alamo T. Computationally efficient nonlinear min-max model predictive control based on volterra series models—Application to a pilot plant. *Journal of Process Control* 2013; **23**(4):543–560.
13. Ukkusuri SV, Ramadurai G, Patil G. A robust transportation signal control problem accounting for traffic dynamics. *Computers & Operations Research* 2010; **37**(5):869–879.
14. Jones LK, Deshpande R, Gartner NH, Stamatidis C, Zou F. Robust controls for traffic networks: the near-Bayes near-Minimax strategy. *Transportation Research Part C: Emerging Technologies* 2013; **27**:205–218.
15. Tettamanti T, Luspay T, Kulcsár B, Péni T, Varga I. Robust control for urban road traffic networks. *IEEE Transactions on Intelligent Transportation Systems* 2014; **15**(1):385–398.
16. Zhong RX, Sumalee A, Pan TL, Lam WHK. Optimal and robust strategies for freeway traffic management under demand and supply uncertainties: an overview and general theory. *Transportmetrica A: Transport Science* 2014; **10**(10):849–877.
17. Liu S, Frejo JRD, Núñez A, De Schutter B, Sadowska A, Hellendoorn J, Camacho EF. Tractable robust predictive control approaches for freeway networks. *Proceedings of the 17th International Conference on Intelligent Transportation Systems*, Qingdao, China, 2014; 1857–1862.
18. Zegeye SK, De Schutter B, Hellendoorn J, Breunese EA, Hegyi A. A predictive traffic controller for sustainable mobility using parameterized control policies. *IEEE Transactions on Intelligent Transportation Systems* 2012; **13**(3):1420–1429.
19. Calafiore GC, Fagiano L. Robust model predictive control via scenario optimization. *IEEE Transactions on Automatic Control* 2013; **58**(1):219–224.
20. Schildbach G, Fagiano L, Frei C, Morari M. The scenario approach for stochastic model predictive control with bounds on closed-loop constraint violations. *Automatica* 2014; **50**(12):3009–3018.
21. Logghe S, Immers LH. Multi-class kinematic wave theory of traffic flow. *Transportation Research Part B: Methodological* 2008; **42**(6):523–541.
22. Lighthill MJ, Whitham GB. On kinematic waves. II. A theory of traffic flow on long crowded roads. *Proceedings of the Royal Society of London. Series A, Mathematical and Physical Sciences* 1955; **229**(1178):317–345.
23. Richards PI. Shock waves on the highway. *Operations Research* 1956; **4**(1):42–51.
24. Messmer A, Papageorgiou M. METANET: a macroscopic simulation program for motorway networks. *Traffic Engineering and Control* 1990; **31**(8–9):466–470.
25. Smulders S. Control of freeway traffic flow by variable speed signs. *Transportation Research Part B: Methodological* 1990; **24**(2):111–132.
26. Papageorgiou M, Kotsialos A. Freeway ramp metering: an overview. *IEEE Transactions on Intelligent Transportation Systems* 2002; **3**(4):271–281.
27. 't Hart J. Comparison of conventional and parameterized MPC for traffic control: A case study. *Master's Thesis*, Delft University of Technology, Delft, Netherlands, 2011.

28. Wang Y, Papageorgiou M, Gaffney J, Papamichail I, Rose G, Young W. Local ramp metering in random-location bottlenecks downstream of metered on-ramp. *Transportation Research Record* 2010; **2178**:90–100.
29. Papageorgiou M, Haj-Salem H, Blosseville JM. ALINEA: a local feedback control law for on-ramp metering. *Transportation Research Record* 1991; **1320**:58–64.
30. Keerthi SS, Gilbert EG. Optimal infinite-horizon feedback laws for a general class of constrained discrete-time systems: stability and moving-horizon approximations. *Journal of Optimization Theory and Applications* 1988; **57**(2):265–293.
31. Mayne DQ, Michalska H. Receding horizon control of nonlinear systems. *IEEE Transactions on Automatic Control* 1990; **35**(7):814–824.
32. Jadbabaie A, Hauser J. On the stability of receding horizon control with a general terminal cost. *IEEE Transactions on Automatic Control* 2005; **50**(5):674–678.
33. Courant R, Friedrichs K, Lewy H. On the partial difference equations of mathematical physics. *IBM Journal of Research and Development* 1967; **11**(2):215–234.
34. Hegyi A. Model predictive control for integrating traffic control measures. *PhD thesis*, Delft University of Technology, Delft, Netherlands, 2004.
35. Kotsialos A, Papageorgiou M, Mangeas M, Haj-Salem H. Coordinated and integrated control of motorway networks via non-linear optimal control. *Transportation Research Part C: Emerging Technologies* 2002; **10**(1):65–84.
36. Frejo JRD, Núñez A, De Schutter B, Camacho EF. Hybrid model predictive control for freeway traffic using discrete speed limit signals. *Transportation Research Part C: Emerging Technologies* 2014; **46**:309–325.
37. Papageorgiou M, Blosseville JM, Haj-Salem H. Modelling and real-time control of traffic flow on the southern part of Boulevard Périphérique in Paris: Part II: coordinated on-ramp metering. *Transportation Research Part A: General* 1990; **24**(5):361–370.